

CURRENT DIFFERENTIAL PILOT RELAYING PROTECTION TECHNIQUE FOR SERIES COMPENSATED LINES USING WAVELET TRANSFORM

4.1. Basic Current Differential Relaying

Current differential relaying is applied to protect many elements of a power system. The simplest example of a current differential relaying scheme is shown in Figure 4.1. The protected element might be a length of circuit conductor, a generator winding, a bus section, a transmission line, etc. From Figure 4.1 it can be seen that current differential relaying is a basic application of Kichorff's Current Law. The relay operates on the sum of the currents flowing in the CT secondary, $I_1 + I_2$. For through current conditions, such as load or an external fault, the currents in the two CT's will be equal in magnitude and opposite in phase (assuming the CT's have the same ratio and are properly connected and neglecting line charging currents in case of Transmission Lines), and there will be no current flow in the relay operate coil [51].

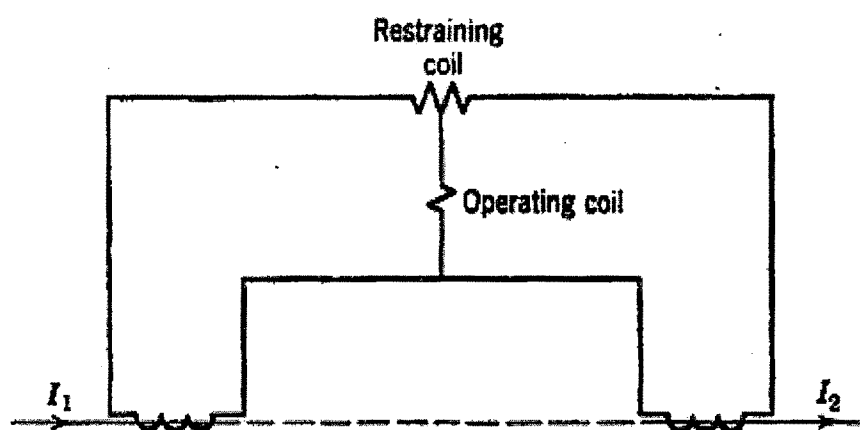


Fig. 4.1 Basic Current Differential Principle
(Where I_1 : Current Entering the Protected Zone, I_2 : Current Leaving the Protected Zone)

In case of short circuit within the protected section between two CT, current will flow through the operating circuit causing the relay to issue a trip command. To improve the selectivity and security of the current differential scheme, it is often designed as a

percentage restraint differential relay. In a percentage restraint current differential relay, the operating current is the differential current through operating coil i.e;

$$I_{\text{operate}} = | I_1 - I_2 | \text{-----} (4.1)$$

This operating current must be greater than the restraining current which is derived from the sum of the magnitude of the individual CT currents. A typical restraint current could be:

$$I_{\text{restraint}} = [| I_1 | + | I_2 |] / 2 \text{-----} (4.2)$$

The operating characteristic of the percentage restraint current differential relay is shown in Figure 4.2.

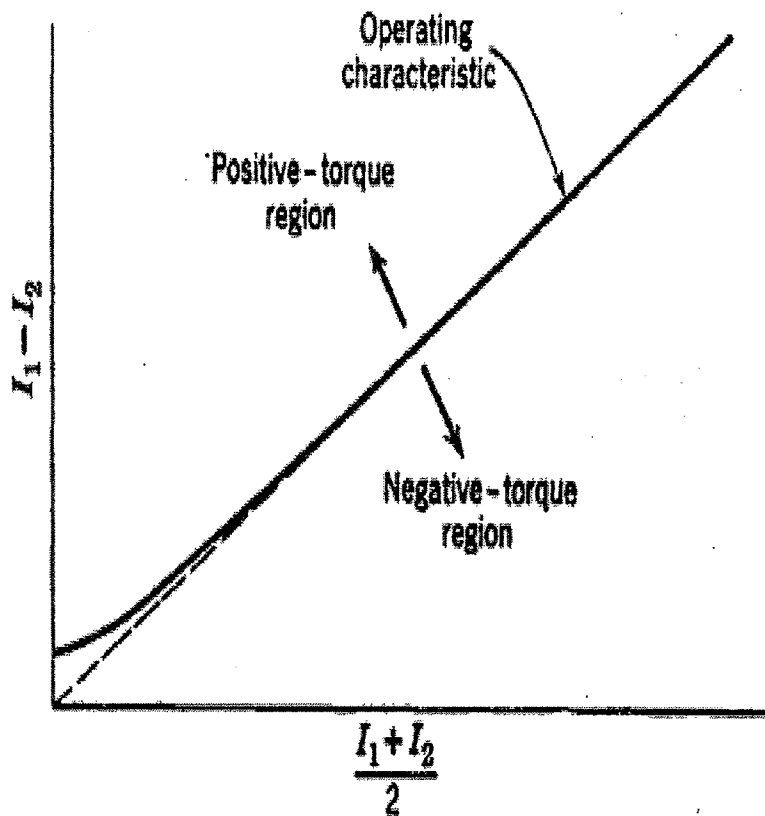


Fig. 4.2 Operating Characteristic of Percentage Restraint Current Differential Relay

4.2 Current Differential Pilot Relay Protection for Transmission Lines

Due to its selectivity, pilot relaying is one of the most popular protections for important transmission lines [52]. The Current Differential Pilot Relay (CDPR) captures the current samples at the terminals of the protected line and then a decision will be made by comparing the local information with the remote one. Under normal operation or external fault (Figure 4.3), the currents measured at the terminals of the protected lines (i.e. entering current and leaving current) equals each other (neglecting line charging currents) and hence the differential current will be zero. For any internal fault (Figure 4.4), these currents will not be equal and further due to reversal of the direction of current from remote ends, results in to differential current (the operating quantity for CDPR) ultimately leading to tripping off the protected line by CDPR.

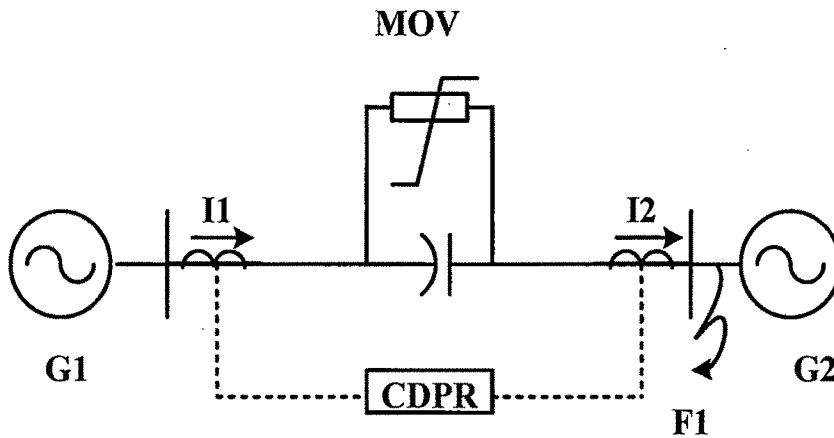


Fig. 4.3 External Fault Case ($I_1 - I_2 = 0$)

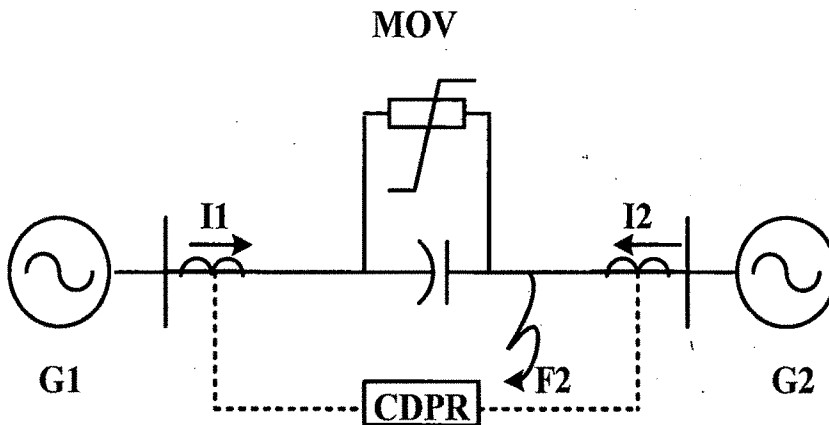


Fig. 4.4 Internal Fault Case ($I_1 - I_2 \neq 0$)

Figure 4.5 presents the characteristic curves of general CDPR [53]. The X and Y -axes present the entering and leaving current, respectively. Under normal case or external fault, leaving current equals entering current; this property is presented by the straight line with 45° . Since there is capacitance in the transmission line, leaving current does not exactly equal entering current, this phenomenon is presented by the dotted line near the 45° line. The active areas in this figure mean that the relay will trip off the line when the compared result falls within these ranges. Obviously, there are dead zones between the dotted line and the active areas where the relay should take action, but it will not. These dead zones are induced by the influence of CT.

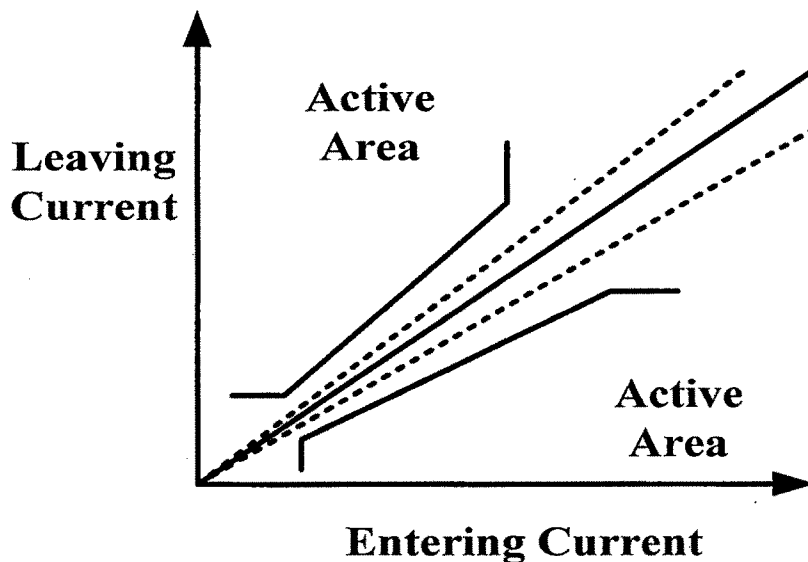


Fig. 4.5 Characteristic Curves for CDPR

4.3 The Proposed Scheme

Transmission line relaying involves three major tasks, namely detection, classification and location of transmission line faults. Fast detection of transmission line faults enables quick isolation of the faulty line from service and, hence, protecting it from the harmful effects of the fault. Classification of faults means identification of the type of fault, and this information is required for fault location and accessing the extent of repair work to be carried out. Fault detection, classification and section identification is a very challenging task for series compensated transmission lines.

Nowadays the trend is to locate faults quickly, reliably and, if possible, without human intervention. This is made directly possible by utilizing fault generated signals [54]. A fault produces a wide spectrum of signals that contains information about the fault distance. These signals are the power frequency component and the transients. The transients can be used in fault detection, classification and location for both repair and protection purposes instead of the power frequency components. This is possible because the fault transients develop much faster and are less dependent on network configuration than the power frequency component.

Because the fault transients are of different frequencies (higher) than the fundamental frequency, the following aspects must be investigated:

- 1) The conditions under which the fault transients will be of sufficient amplitude and frequency for fault detection, classification and location.

- 2) The transients are affected by the network itself during their propagation in fault loop. The line parameters are not constant for different transient frequencies and ground impedances. Also, the way by which the transient approaches to the substation might be influential. The return path of the fault current will depend on the overhead ground wires, the network configuration (mainly the connected lines) and also on the type of neutral grounding.

- 3) The measurements of the transients are usually performed by instrument transformers, which are designed for 50 Hz. Use of these devices for fault transients might not be as accurate as for 50 Hz. The fault transients can be obtained from the measurement of voltages and current at the substation.

- 4) Fault signals are of the special “non-stationary signal” type. In practice these signals also contain a lot of noise and transients other than the needed component. The transient might also be of small in amplitude and length. Therefore, for good fault estimation, a suitable signal processing tool must be chosen.

With this much preliminary discussion about the fault generated high frequency transients it's evident that they can be used for detection, classification and location of the faults on any kind of transmission network. The further section discusses the suggested unit protection method (CDPR) for detection, discrimination, classification of faults for series compensated transmission line using wavelet transform as a signal processing tool where instead of directly comparing the currents captured from CT, "the fault generated high frequency transients typical signature as it appears after processing post fault signals at relaying terminals at the ends of the transmission line"- which will further be identified as "fault spike/s" in this work- is used as a control variable so that the influence of line capacitance will be reduced. Also, the proposed technique does not require an accurate replica of the primary current; the purpose of CT in this approach is to provide enough strength for detecting jumps. As a result, this novel approach can improve the sensitivity by enlarging the active areas (Figure 4.5).

As discussed in detail in chapter-2 Both the Fourier transformation (FT) and wavelet transformation (WT) are used to expand functions in terms of a set of basic functions. In WT, these basic functions are generated by a specific function known as "mother function" that must oscillate and decays quickly to zero. Unlike FT, WT enables time localization of different frequency components of a given signal, but FT cannot. Discrete wavelet transform (DWT) is mostly preferred for application of wavelets in order to achieve objectives related to detection, classification and discrimination of faults.

Actually, DWT can be implemented by filter banks (i.e., involving successive pairs of high-pass and low-pass filters at each scaling stage in the WT). It means the approximations are the high-scale, low-frequency components of the signal, and the details are the low-scale, high-frequency components. Based on this multi-resolution feature, WT is often used to detect sudden changes in power system. Since wavelet analysis is a very sensitive tool for detection of sudden change in power system condition, it will be used to identify the faulted phase and classify fault type by examining the appearing fault spike. Figure 4.6 shows flow chart of the proposed scheme.

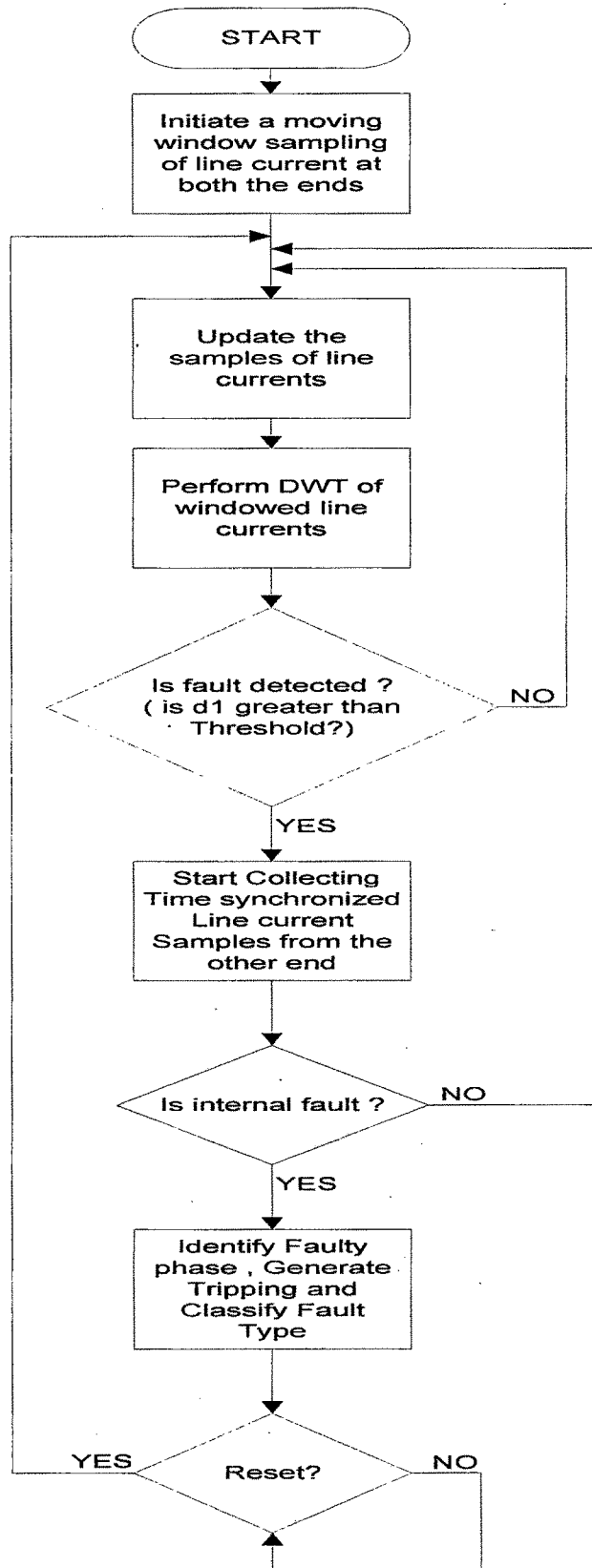


Fig.4.6 Flow Chart of Proposed Scheme

4.4 Working of the Scheme and Simulation Studies

The objective of following section is to describe how wavelet transform is used in order to analyze the fault generated signals and find out the various threshold coefficients which will be used by algorithm of the CDPR relay as a control variable for detection, discrimination, classification of the faults and subsequent tripping of the protected line as depicted by the proposed scheme flow chart in Figure 4.6.

When the current signals captured at both the ends of the lines are analyzed by performing Discrete Wavelet Transform (DWT) using Daubechies-4 (db4) as a mother wavelet, It has been observed that whenever there is sudden change in the magnitude of the current due to any type of the fault/change, the level-6 detail coefficients (d6) is experiencing a sudden rise in numbers and magnitude. This peculiar characteristic of the wavelet transform enables us to take various decisions regarding the systems present status as follows:

4.4.1 Detection of the Fault and Identification of Faulty Phase

DWT transform of all the three line current samples (captured at a sampling frequency of 20 KHZ) are performed. If the values of d6 coefficients are higher then set threshold, (Threshold decision making procedure will be explained ahead) the decision is taken that the particular phase is faulty.

4.4.2 Discriminating between Internal and External Fault

Irrespective of the location of the fault, i.e. external to the line or on the line DWT will detect all the fault spikes, hence in order to distinguish between internal and external fault the approach uses pattern of the spikes as decision making factor for internal or external fault. As it will be clear from the Fig.4.7 and Fig.4.8 that in the event of the external fault, spike pattern is identical for line currents at the both the ends while for internal fault, the pattern becomes mirror image of each other. Hence once the fault detection is done then immediately its discrimination as internal fault or external fault is done.

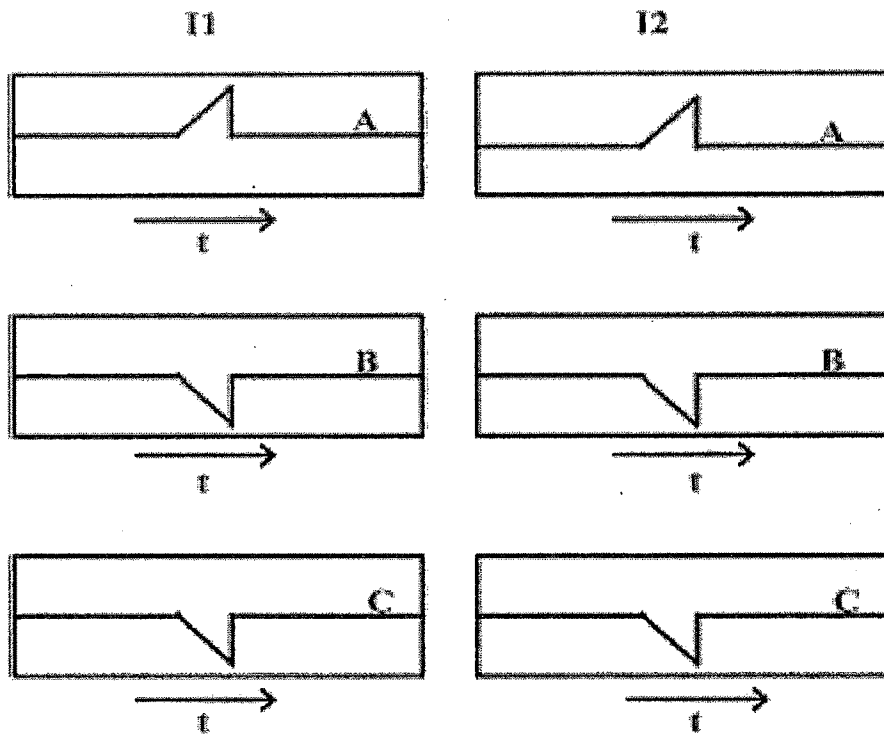


Fig.4.7 Pattern of Spikes at the end of Transmission lines for the case of External Fault

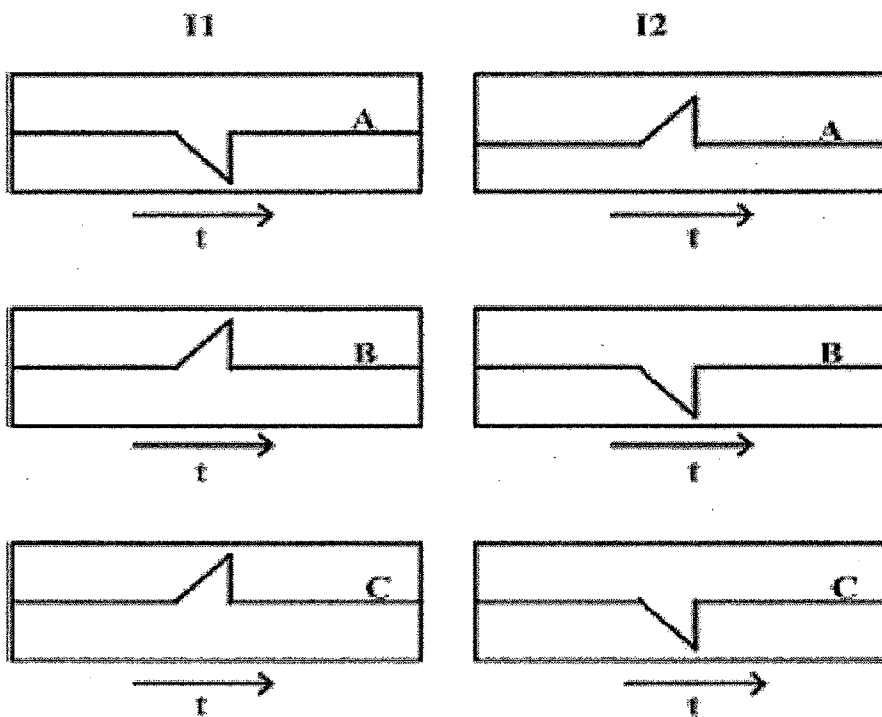


Fig.4.8 Pattern of Spikes at the end of Transmission lines for the case of Internal Fault.

4.4.3 Classification of Fault Type

On the successful detection and discrimination of the fault, the approach checks for the presence of the spikes in zero sequence currents at relaying points above a predetermined threshold value in order to distinguish between double line fault and double line to ground fault (in order to confirm involvement of the ground in detected fault). The presence of the d6 coefficient above a threshold for zero sequence current implies the involvement of the ground in to the fault. Table 4.1 gives quick idea about the approach for faulted phase detection and fault classification.

Table 4.1 Fault Detection and Classification

Fault Type	Value of d6 Coefficients above Threshold for Ia	Value of d6 Coefficients above Threshold for Ib	Value of d6 Coefficients above Threshold for Ic	Value of d6 Coefficients above Threshold for I0
A-g	Y	N	N	Y
B-g	N	Y	N	Y
C-g	N	N	Y	Y
A-B	Y	Y	N	N
B-C	N	Y	Y	N
A-C	Y	N	Y	N
A-B-g	Y	Y	N	Y
B-C-g	N	Y	Y	Y
A-C-g	Y	N	Y	Y
A-B-C	Y	Y	Y	N
A-B-C-g	Y	Y	Y	Y

(N-No, Y-Yes)

4.4.4 Deciding the Thresholds and Simulation studies

In order to evaluate the robustness of the proposed scheme extensive fault simulation studies is carried out on a two terminal transmission line model simulated in MATLAB with a variable series compensation placed at the middle of the line. The transient fault studies are carried out using the well-known MATLAB (SIMPOWERSYSTEMS BLOCKSET) program. The performance of the proposed technique is analyzed for a large test data set (30,000) considering a wide variation in system condition along with a change in the source impedance. The simulation studies

carried out in this work is based on the ideas, methods and parameters used for simulation studies in the work reported in [67].

The model used for simulation studies in MATLAB is shown in Figure 3.6. The transmission line has been represented using the distributed parameters line. The power system comprises of two sources, series capacitor (located at midpoint of the line) and its associated components. The system parameters used has been given in Table 3.1. Over-voltage protection of series capacitor is provided by MOV and parallel power gap. The MOV is protected by C.B. operation against its energy dissipation capacity. The Series capacitor is designed to vary its compensation between 25% minimum to a maximum of 75%.

To test the suggested scheme the fault simulation studies have been carried out under wide variation of load angle, fault inception angle, fault resistance and fault locations. The different values of fault type, load angle, fault inception angle, fault resistance and fault positions (before and after the Series Capacitor), which have been chosen for this study, are as follows:

- (i) Fault Type: a-g, b-g, c-g, a-b, b-c, c-a, a-b-g, b-c-g, c-a-g, a-b-c/a-b-c-g
- (ii) Load angle: 10° , 20° , and 30°
- (iii) Fault inception angle: 0° , 45° , 80° , 115°
- (iv) Fault resistance: 0.01Ω , 1Ω , 50Ω , 100Ω .
- (v) Fault Locations: 20% & 40% (Before the Series Capacitor),
60% & 80% (after the Series Capacitor)

Thus, $10 \times 3 \times 4 \times 4 \times 4 = 1920$ combinations of above mentioned parameters have been selected for a single compensation level (X_c) with a fixed value of source impedance Z_{G1} and Z_{G2} at two ends of the transmission line. A total of 15 different cases have been generated by varying the said two parameters. Hence, $1920 \times 15 = 28800$ test cases are simulated. In addition 1200 case studies of external faults are also simulated. Table 4.2 shows Simulation parameters.

Table 4.2 Simulation Parameters

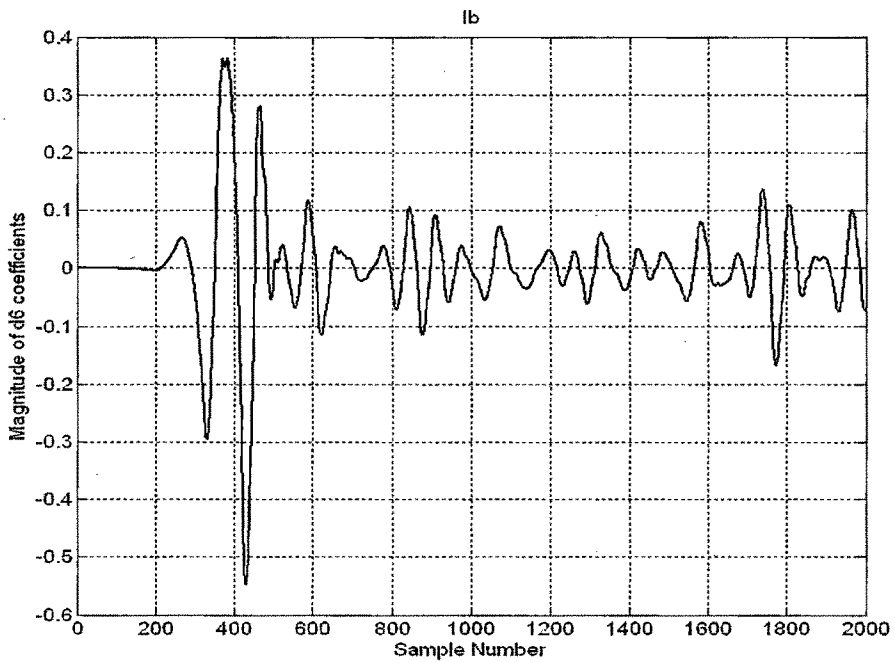
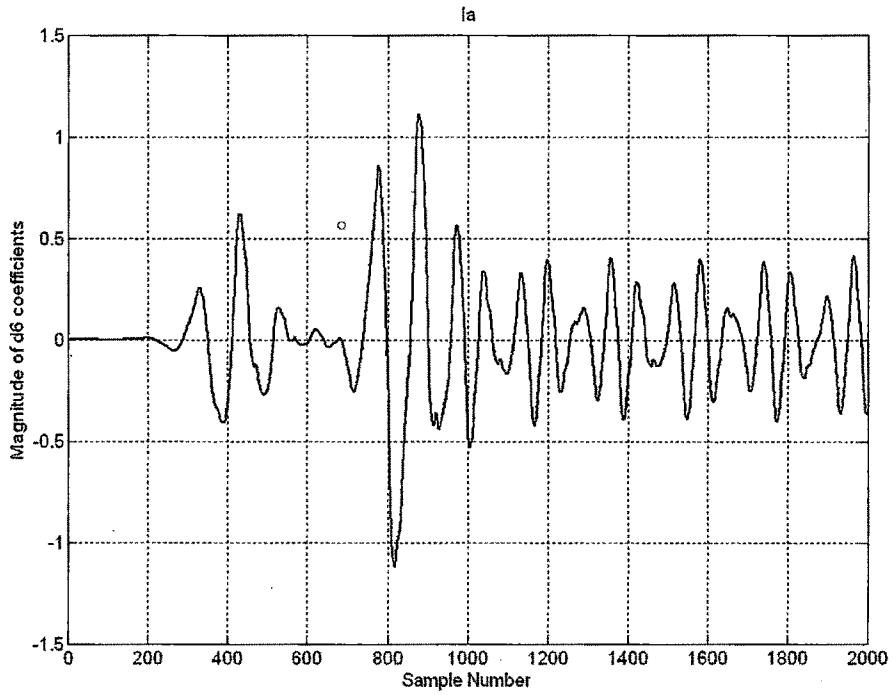
Simulation Time	0.1 Sec (Five Cycles)
Sampling Frequency	20 KHZ
Simulation Starts	T=0 Sec (0 th Sample)
Fault is Applied at	T=0.01 Sec (200 th Sample)
Fault is removed at	T=0.1 Sec (2000 th Sample)
Simulation Ends	T=0.1 Sec (2000 th Sample)

Based on to total test cases analyzed an heuristic approach is selected and threshold value for the level-6 coefficient (d6) is selected as “0.5” for detecting spikes in line currents and a threshold value of level-6 coefficient (d6) is selected as “0.00001” for detecting spikes in zero sequence currents. (These thresholds are for the case of 50% series compensation and 100% source impedances for the both sources. A separate thresholds need to be worked out for different compensation levels with different source impedance combinations through the same approach.)

Next section will be demonstrating some case studies of fault simulations done considering the suggested scheme.

4.4.5 Some Case Studies and related Discussions

(1) $X_c=50\%$, $ZG1=100\%$, $ZG2=100\%$, A-B Fault at 60KM from Bus-B1, $R_f=1 \Omega$



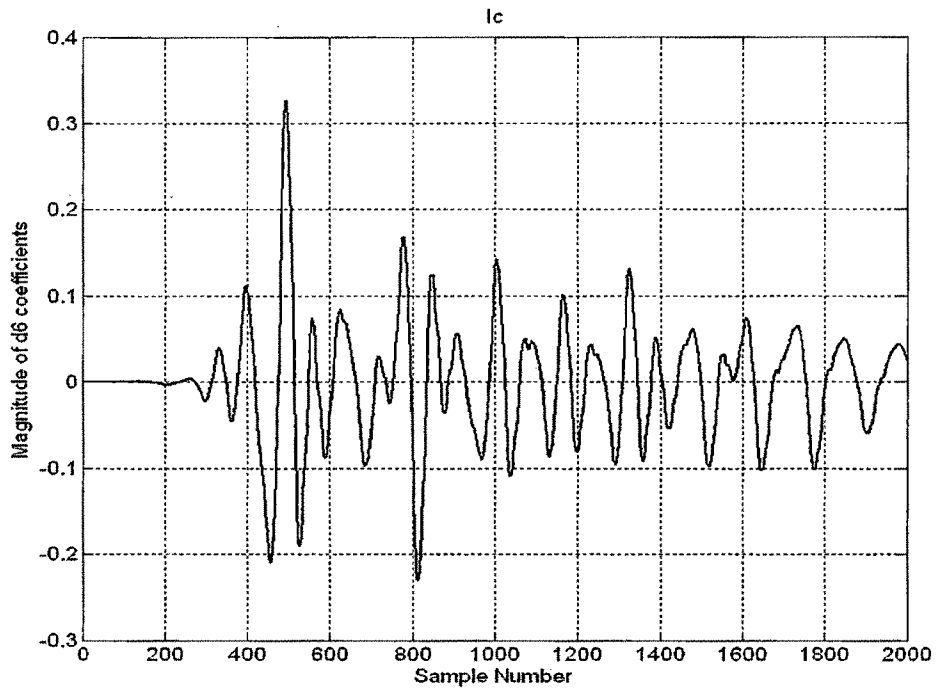
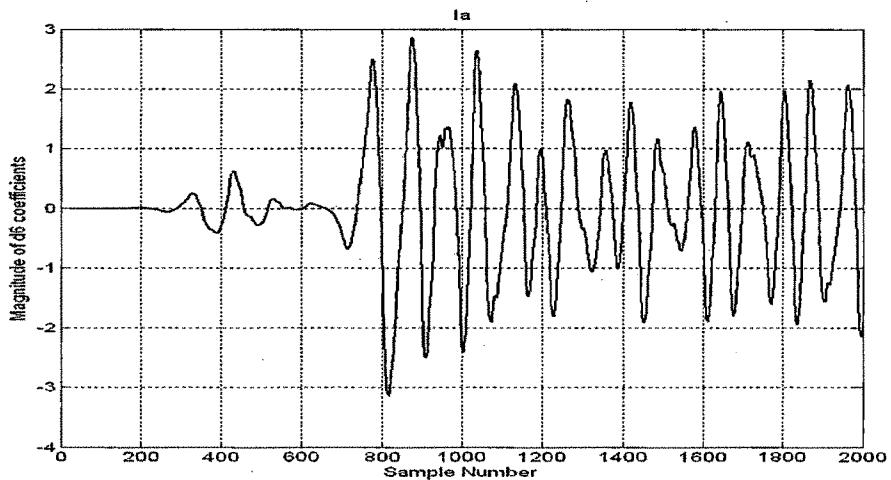


Fig.4.9 Plots showing magnitudes of fault spikes for A-B fault at 20% Line Length

From the plots (Figure 4.9) its evident that the magnitude of level 6 detail coefficients exceeding the set threshold in phase A,B and hence the scheme will detect fault as A-B fault and will take further relaying decision accordingly.

(2) $X_c=50\%$, $Z_{G1}=100\%$, $Z_{G2}=100\%$, A-B-C Fault at 120 KM from Bus-B1, $R_f=0.01 \Omega$



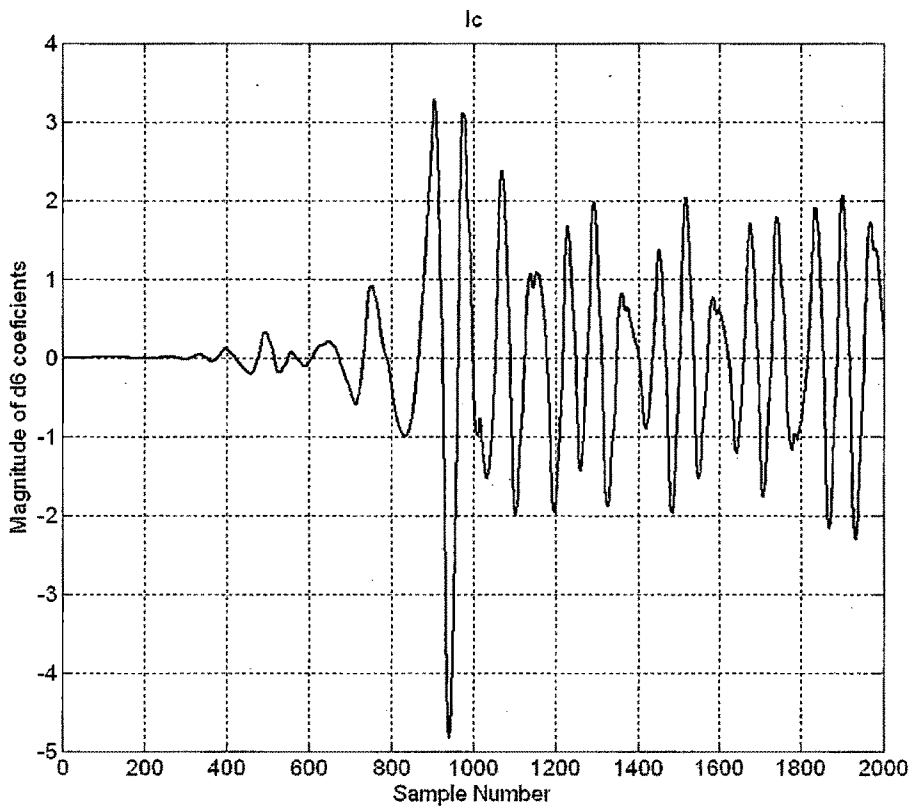
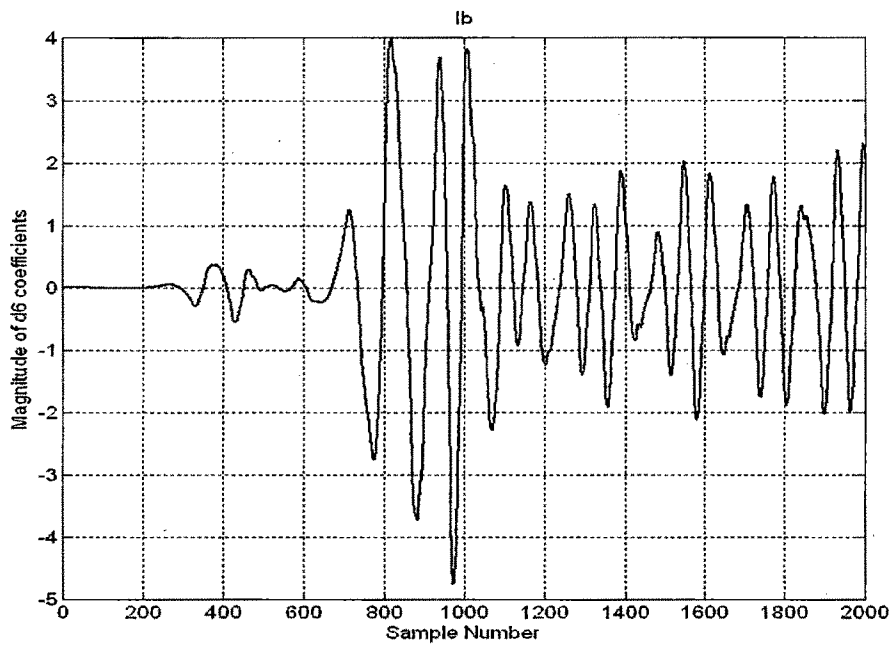
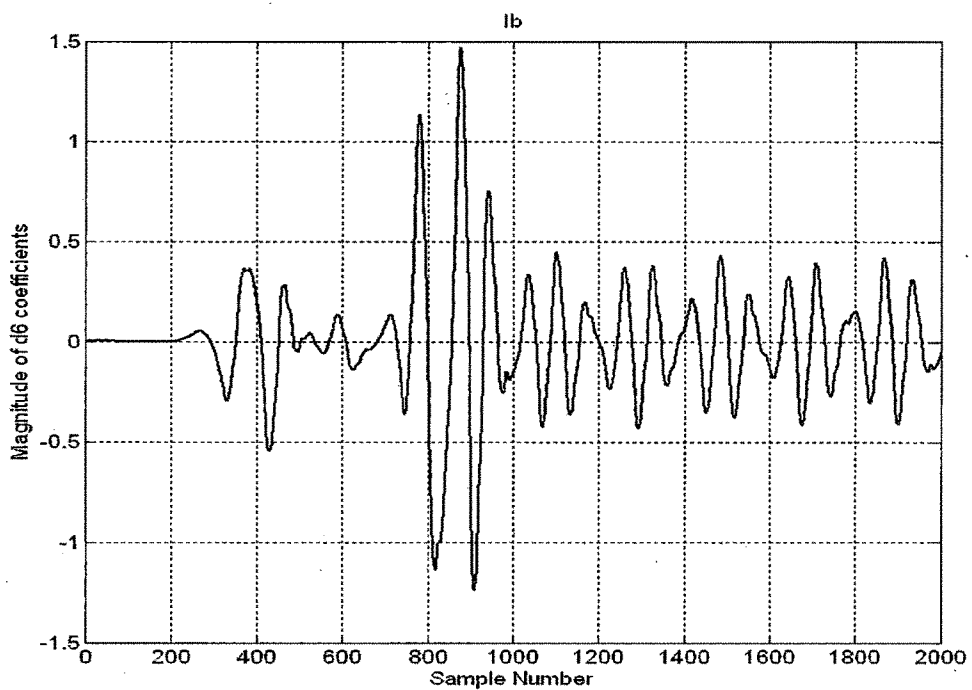
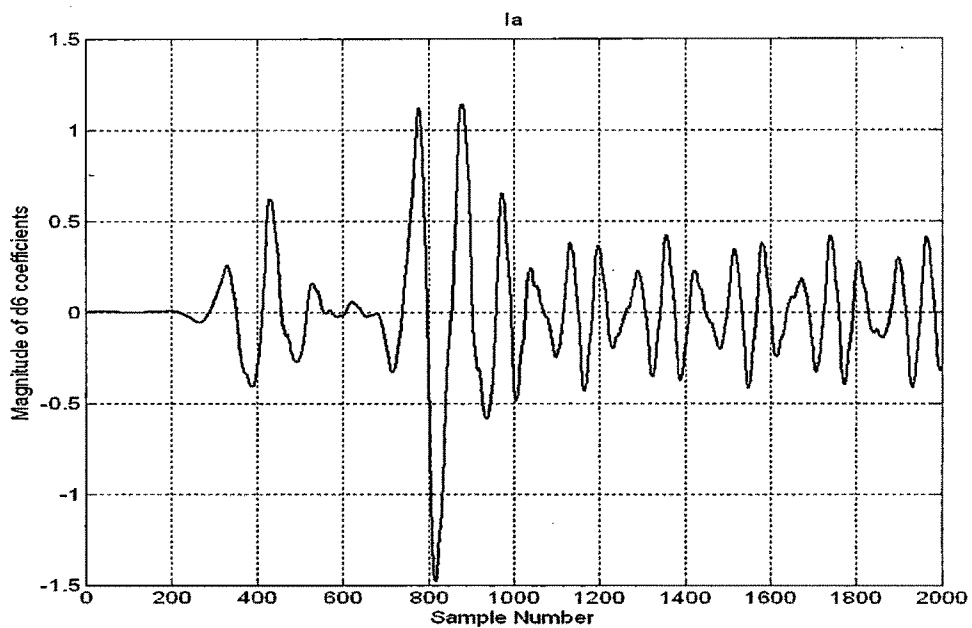


Fig.4.10 Plots showing magnitudes of fault spikes for A-B-C fault at 40% Line Length

From the plots (Figure 4.10) it's evident that the magnitude of level 6 detail coefficients exceeding the set threshold in all the phases hence the scheme will detect fault as A-B-C fault and will take further relaying decision accordingly.

(3) $X_c=50\%$, $Z_{G1}=100\%$, $Z_{G2}=100\%$, A-B-C Fault at 180 KM from Bus-B1, $R_f=100 \Omega$



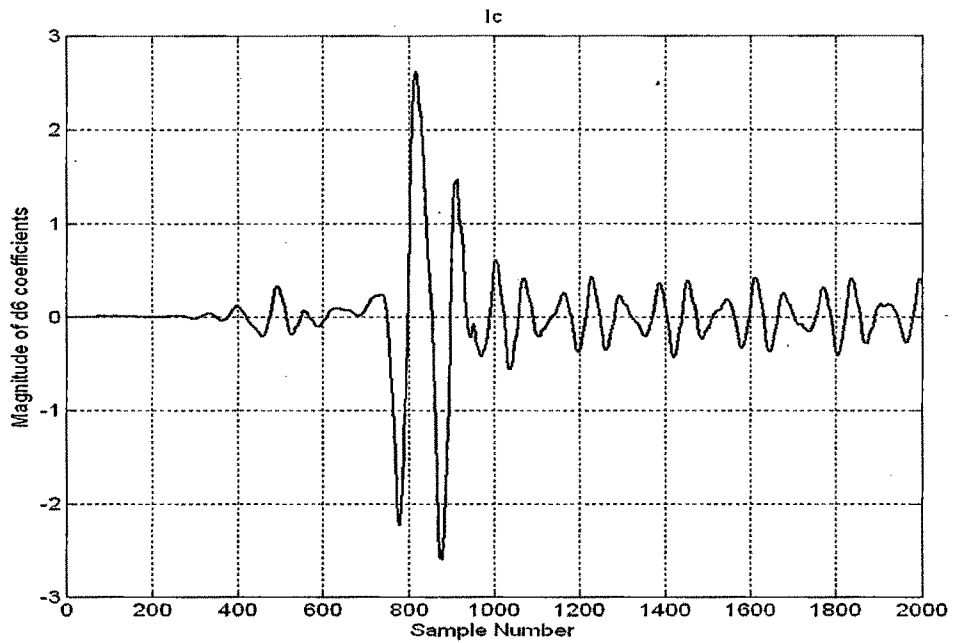
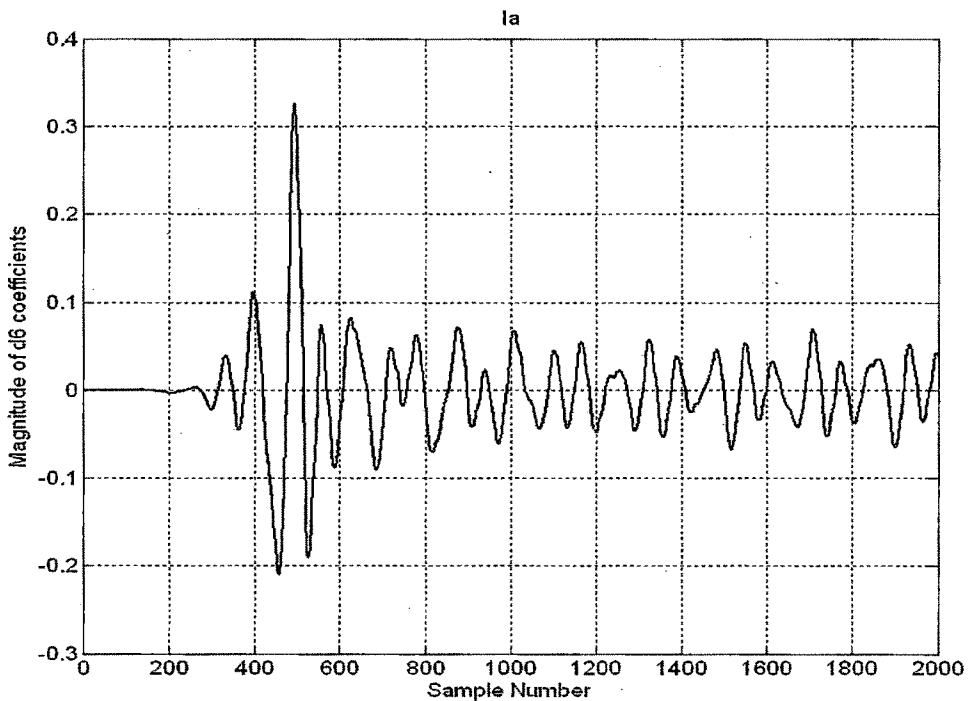


Fig.4.11 Plots showing magnitudes of fault spikes for A-B-C fault at 60% Line Length

From the plots (Figure 4.11) it's evident that the magnitude of level 6 detail coefficients exceeding the set threshold in all the phases hence the scheme will detect fault as A-B-C fault and will take further relaying decision accordingly.

(4) $X_c=50\%$, $Z_{G1}=100\%$, $Z_{G2}=100\%$, B-C Fault at 180 KM from Bus-B1, $R_f=0.01 \Omega$



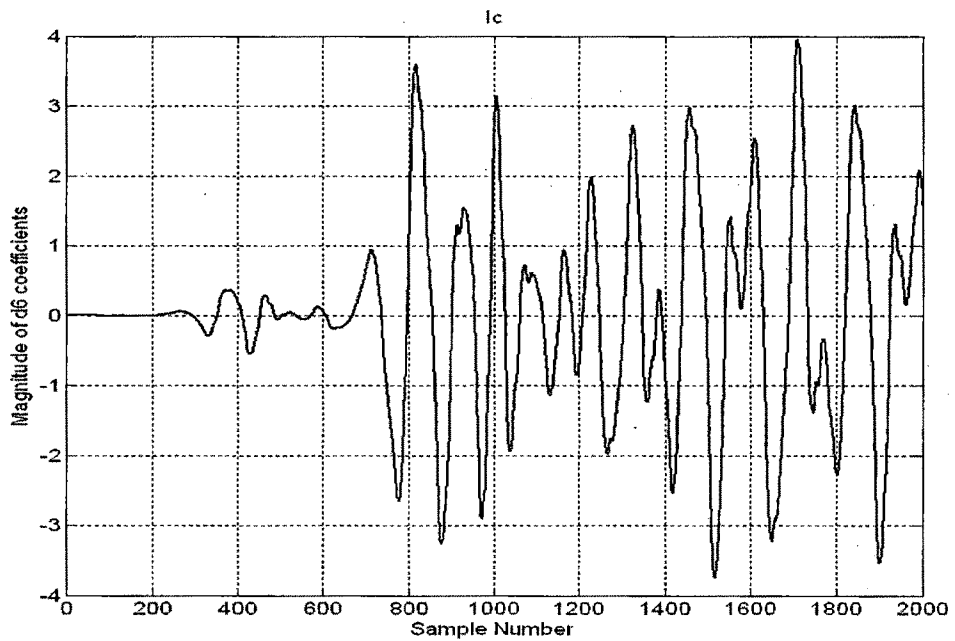
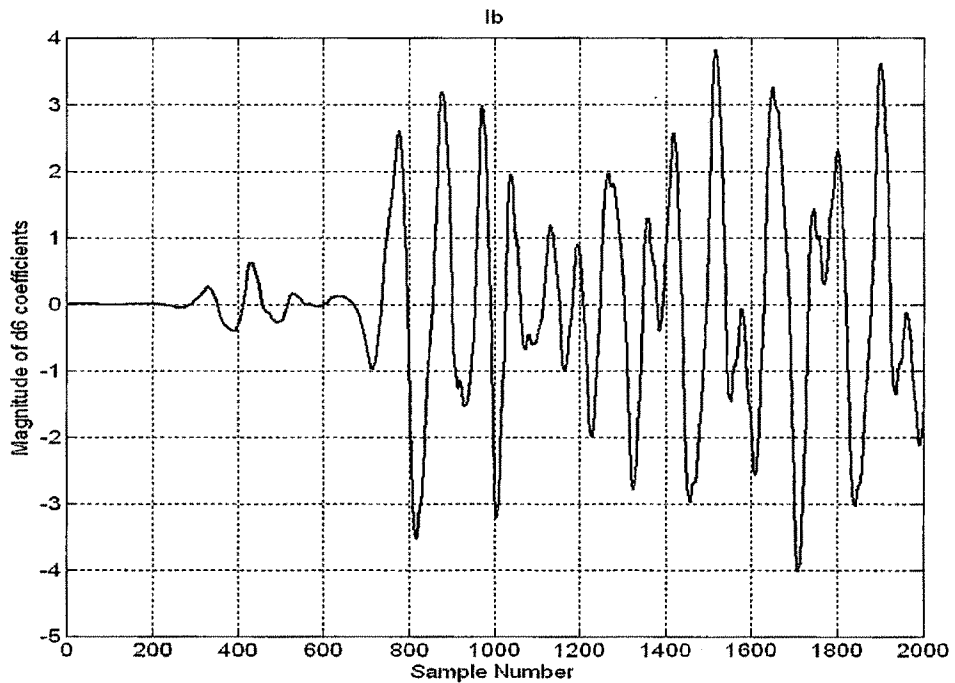


Fig.4.12 Plots showing magnitudes of fault spikes for B-C fault at 60% Line Length

From the plots (Figure 4.12) it's evident that the magnitude of level 6 detail coefficients exceeding the set threshold in B, C phases hence the scheme will detect fault as B-C fault and will take further relaying decision accordingly.

(5) $X_c=50\%$, $Z_{G1}=100\%$, $Z_{G2}=100\%$, A-C Fault at 240 KM from Bus-B1, $R_f=100 \Omega$

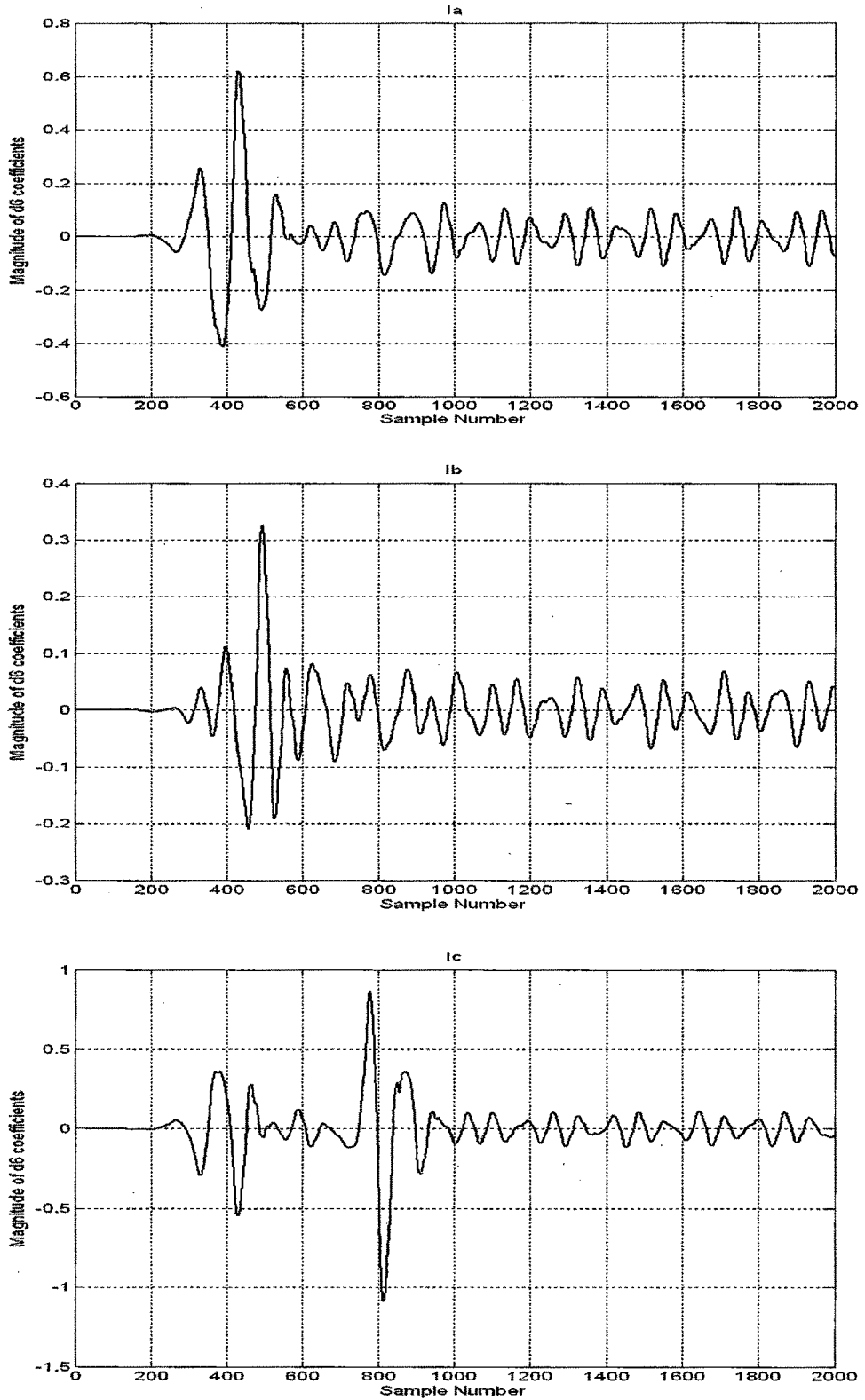
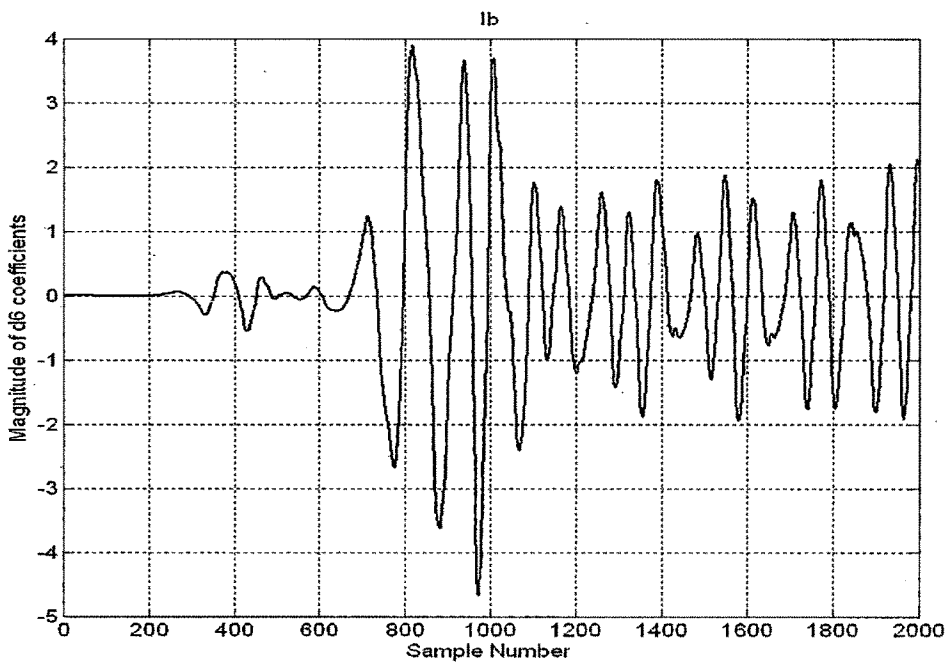
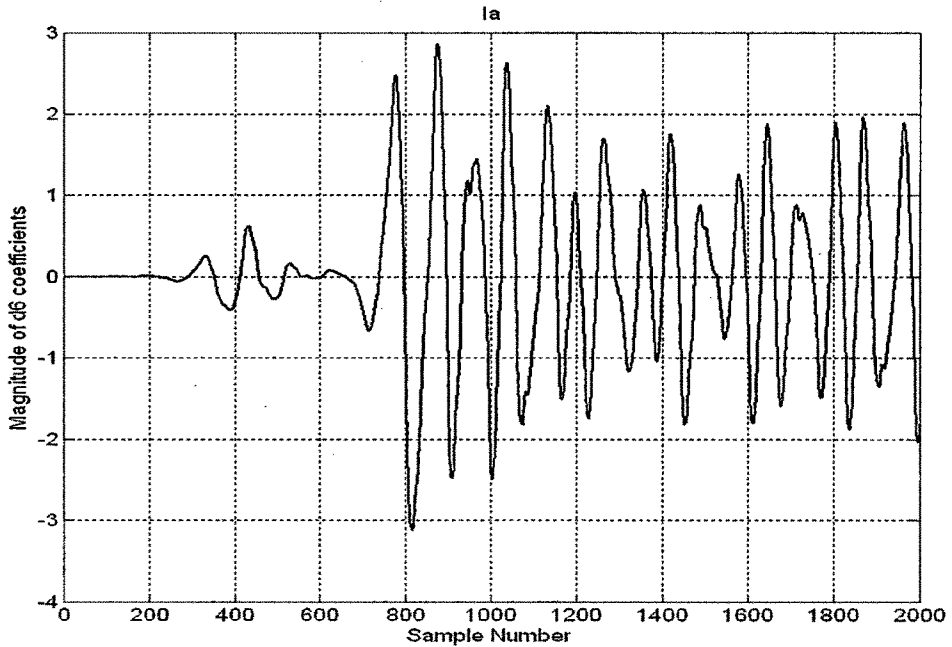


Fig.4.13 Plots showing magnitudes of fault spikes for A-C fault at 80% Line Length

From the plots (Figure 4.13) it's evident that the magnitude of level 6 detail coefficients exceeding the set threshold in A, C phases hence the scheme will detect fault as A-C fault and will take further relaying decision accordingly.

(6) $X_c=50\%$, $Z_{G1}=100\%$, $Z_{G2}=100\%$, A-B-C Fault at 240 KM from Bus-B1, $R_f=1 \Omega$



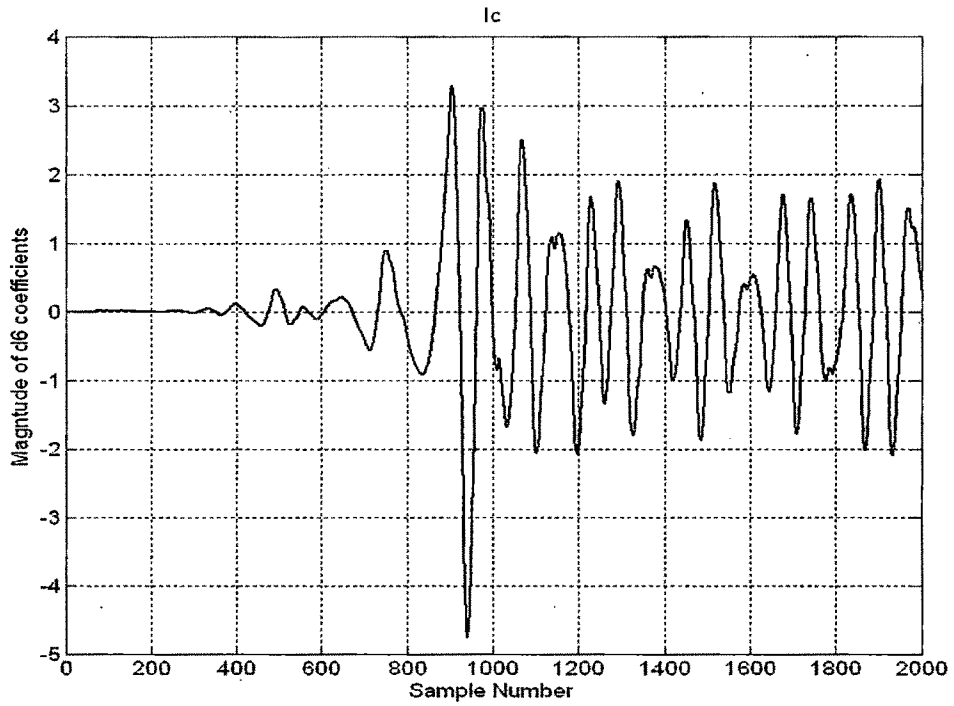
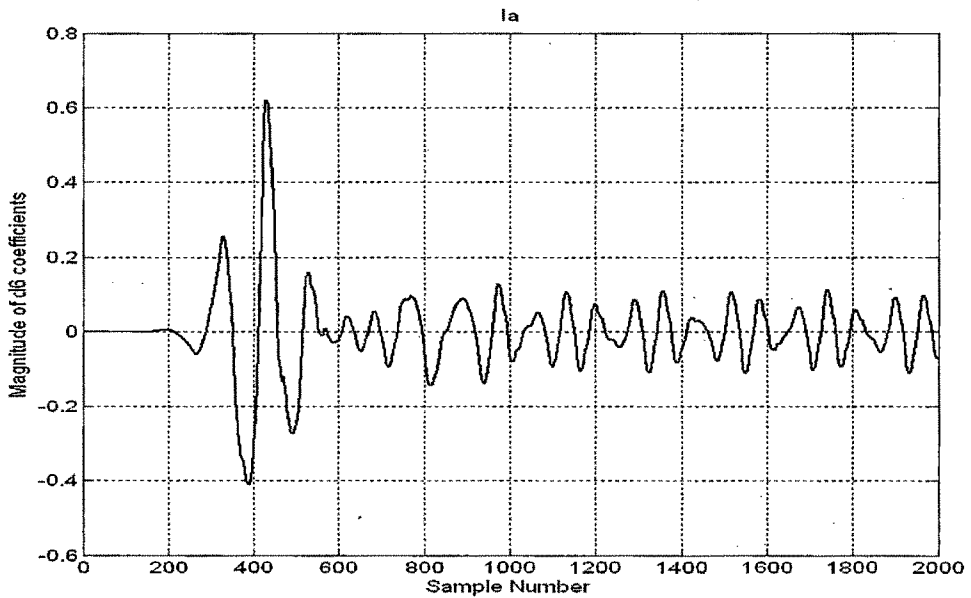


Fig.4.14 Plots showing magnitudes of fault spikes for A-B-C fault at 80% Line Length

From the plots (Figure 4.14) it's evident that the magnitude of level 6 detail coefficients exceeding the set threshold in all the phases hence the scheme will detect fault as A-B-C fault and will take further relaying decision accordingly.

(7) $X_c=50\%$, $ZG1=100\%$, $ZG2=100\%$, A-B-g Fault at 240 KM from Bus-B1, $R_f = 100 \Omega$



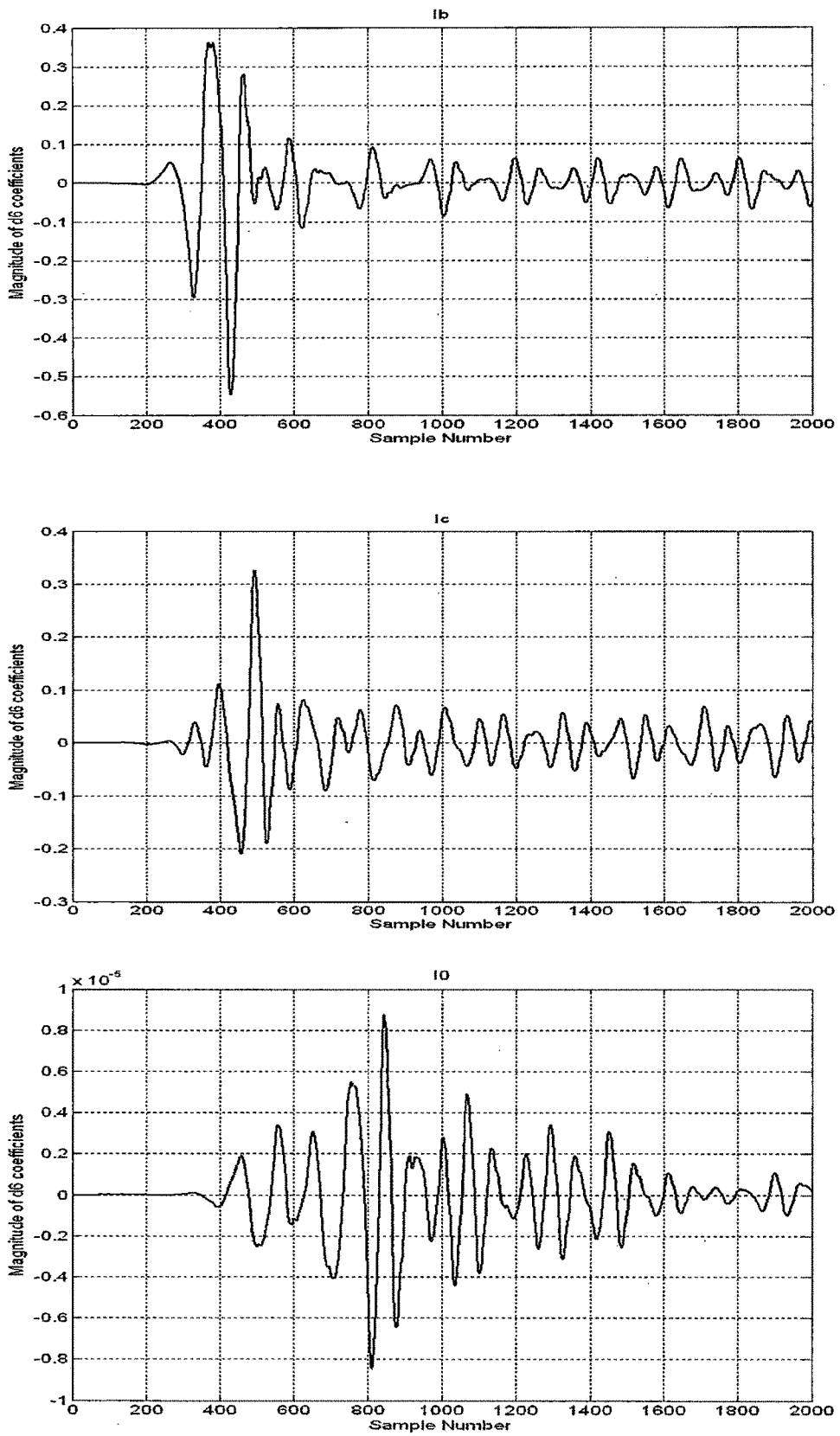
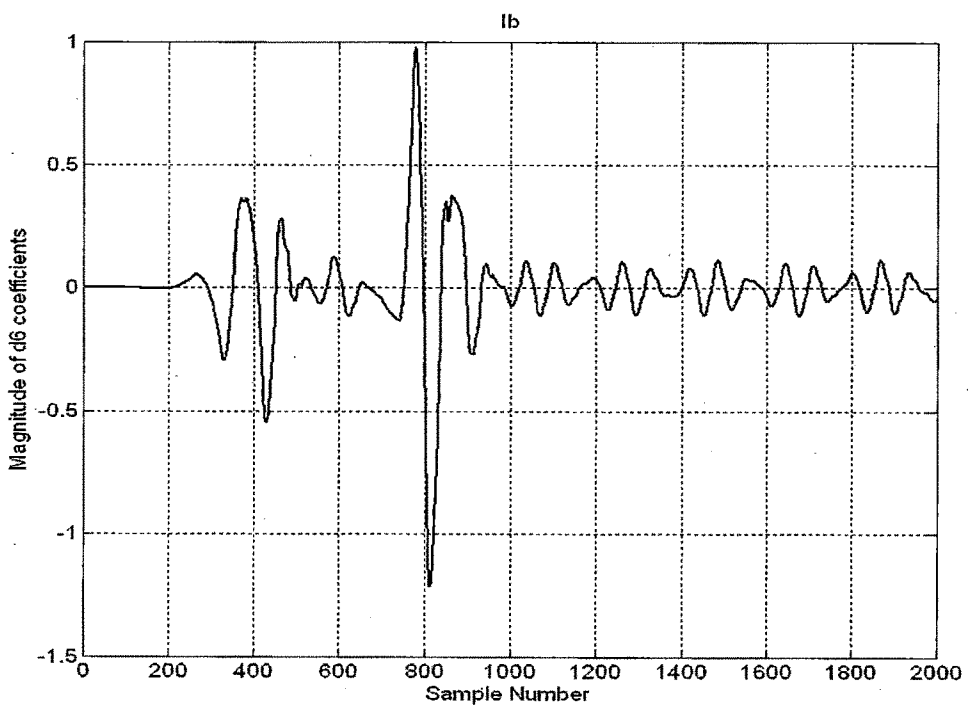
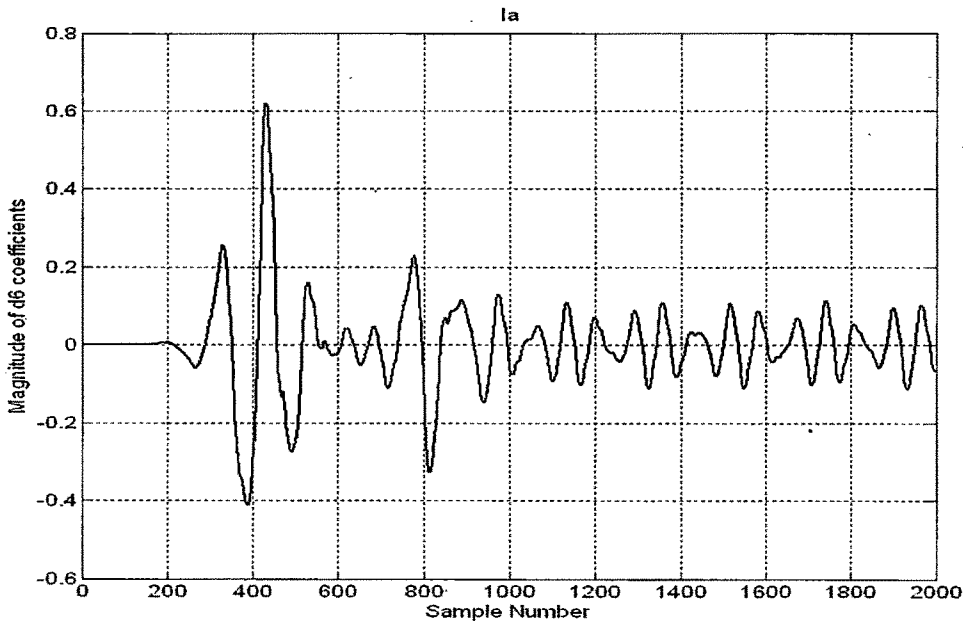


Fig.4.15 Plots showing magnitudes of fault spikes for A-B-g fault at 80% Line Length

From the plots (Figure 4.15) it's evident that the magnitude of level 6 detail coefficients exceeding the set threshold in A,B phases and zero sequence current, hence the scheme will detect fault as A-B-g fault and will take further relaying decision accordingly.

(8) $X_c=50\%$, $Z_{G1}=100\%$, $Z_{G2}=100\%$, A-B-C-g Fault at 60 KM from Bus-B1, $R_f=100\ \Omega$



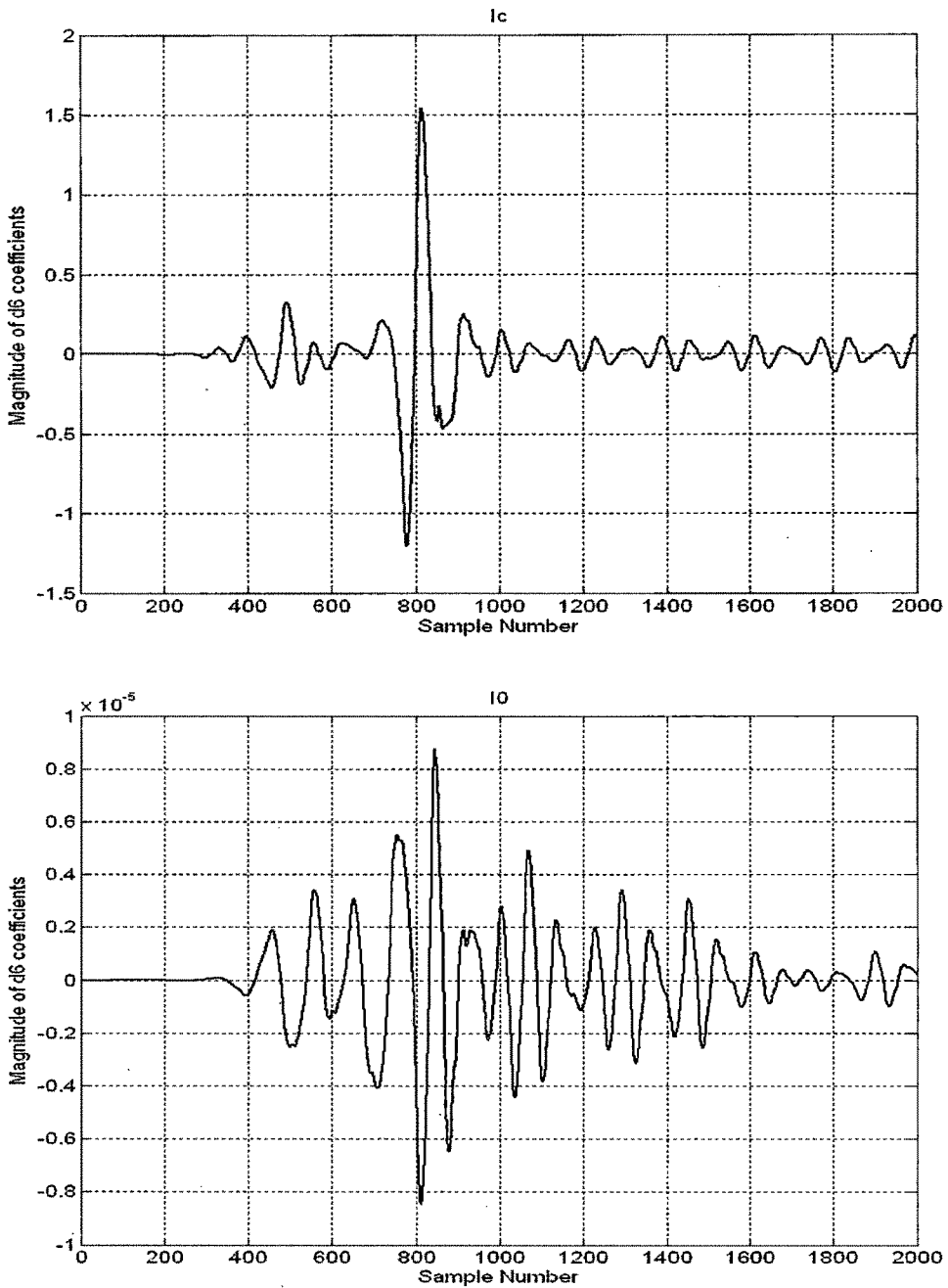


Fig.4.16 Plots showing magnitudes of fault spikes for A-B-C-g fault at 20% Line Length

From the plots (Figure 4.16) it's evident that the magnitude of level 6 detail coefficients exceeding the set threshold in all the phases and zero sequence current, hence the scheme will detect fault as A-B-C-g fault and will take further relaying decision accordingly.

(9) $X_c=50\%$, $Z_{G1}=100\%$, $Z_{G2}=100\%$, A-B-C Fault at 150 KM from Bus-B1, $R_f=0.01 \Omega$
 (On the left of Series Capacitor)

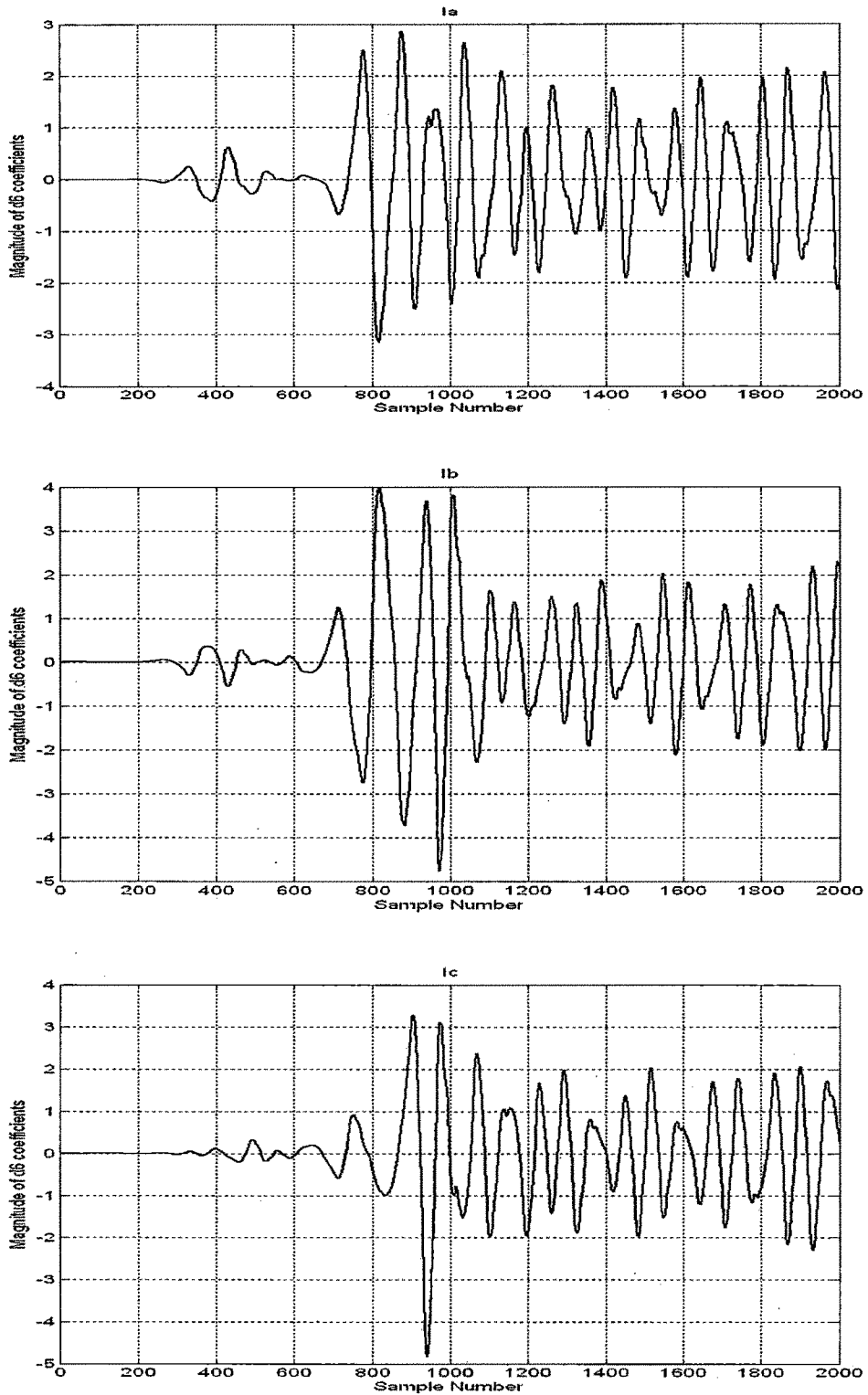


Fig.4.17 Plots showing magnitudes of fault spikes for A-B-C fault at Middle of Line

From the plots (Figure 4.17) it's evident that the magnitude of level 6 detail coefficients exceeding the set threshold in all the phases, hence the scheme will detect fault as A-B-C fault and will take further relaying decision accordingly.

(10) $X_c=50\%$, $Z_{G1}=100\%$, $Z_{G2}=100\%$, A-B-C Fault at 150 KM from Bus-B1, $R_f=0.01 \Omega$
 (On the right of Series Capacitor)

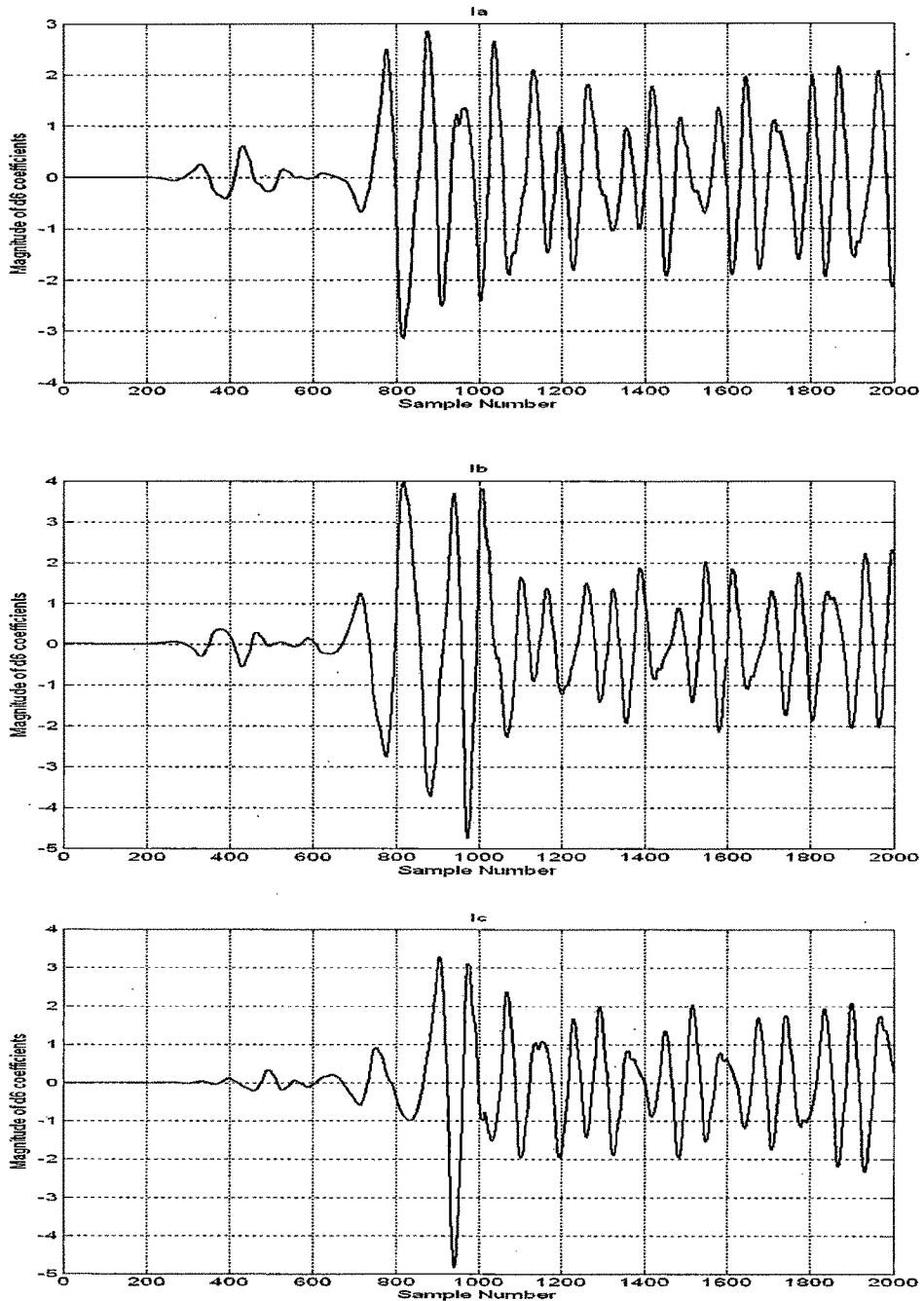


Fig.4.18 Plots showing magnitudes of fault spikes for A-B-C fault at Middle of Line

From the plots (Figure 4.18) it's evident that the magnitude of level 6 detail coefficients exceeding the set threshold in all the phases, hence the scheme will detect fault as A-B-C fault and will take further relaying decision accordingly.

(11) $X_c=50\%$, $Z_{G1}=100\%$, $Z_{G2}=100\%$, A-B Fault between Bus-B2 and Source G2, $R_f=0.01 \Omega$ (External Fault)

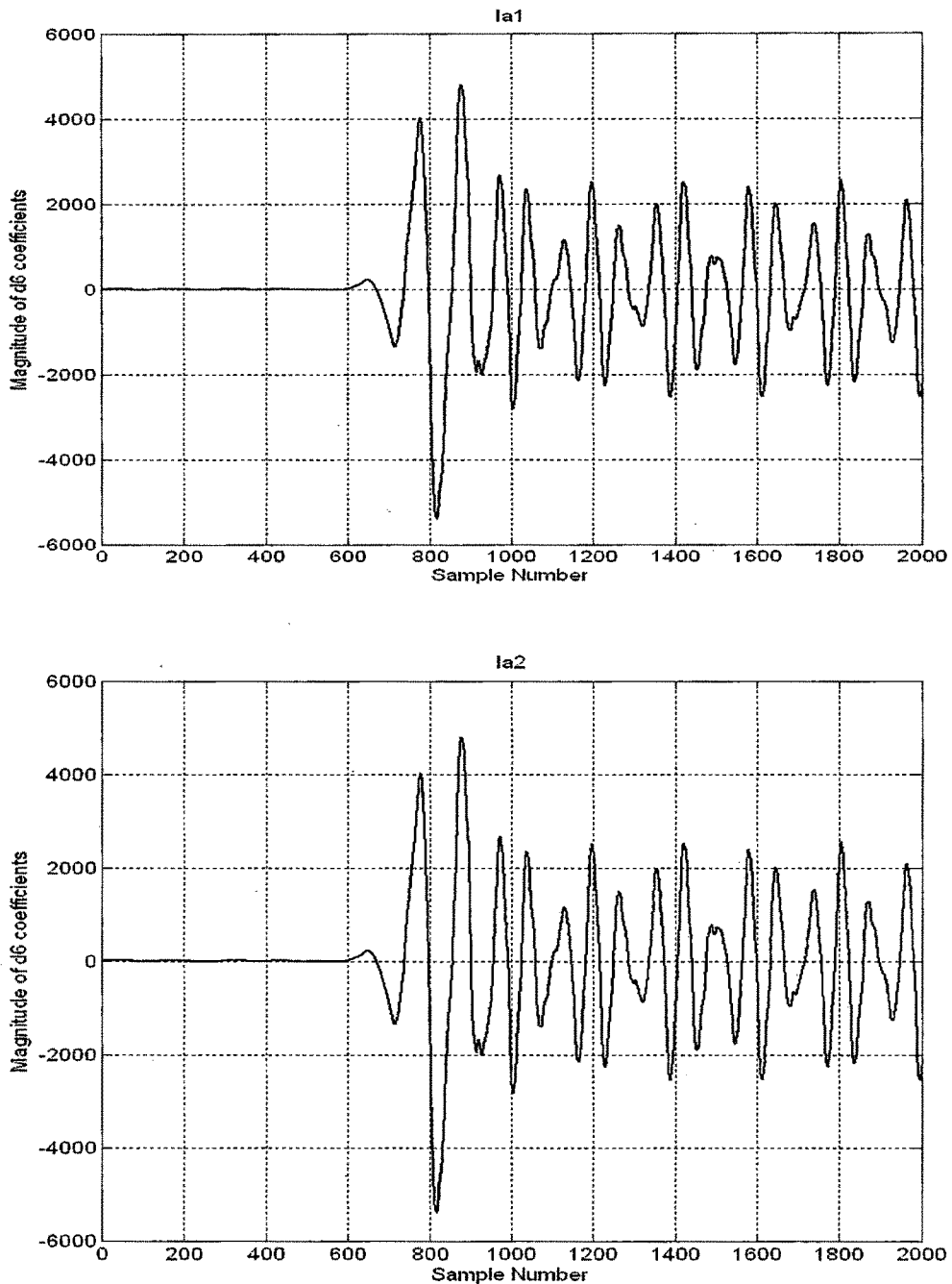


Fig.4.19 Plots showing magnitudes of fault spikes for A- Phase on both the ends for A-B External Fault

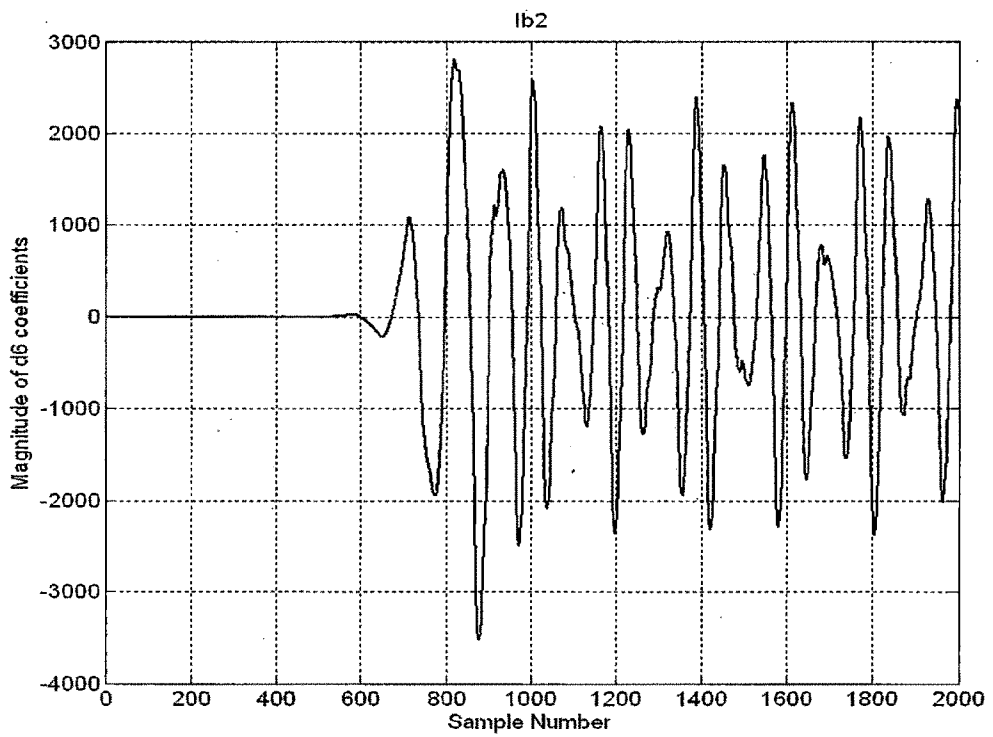
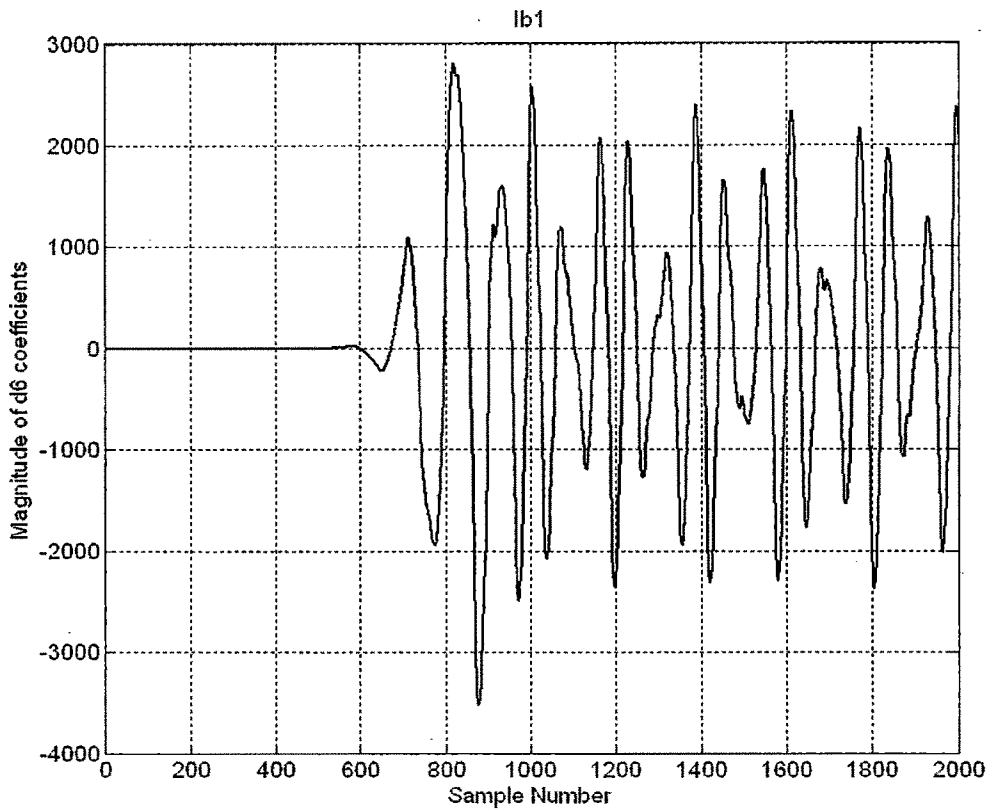


Fig.4.20 Plots showing magnitudes of fault spikes for B- Phase on both the ends for A-B External Fault

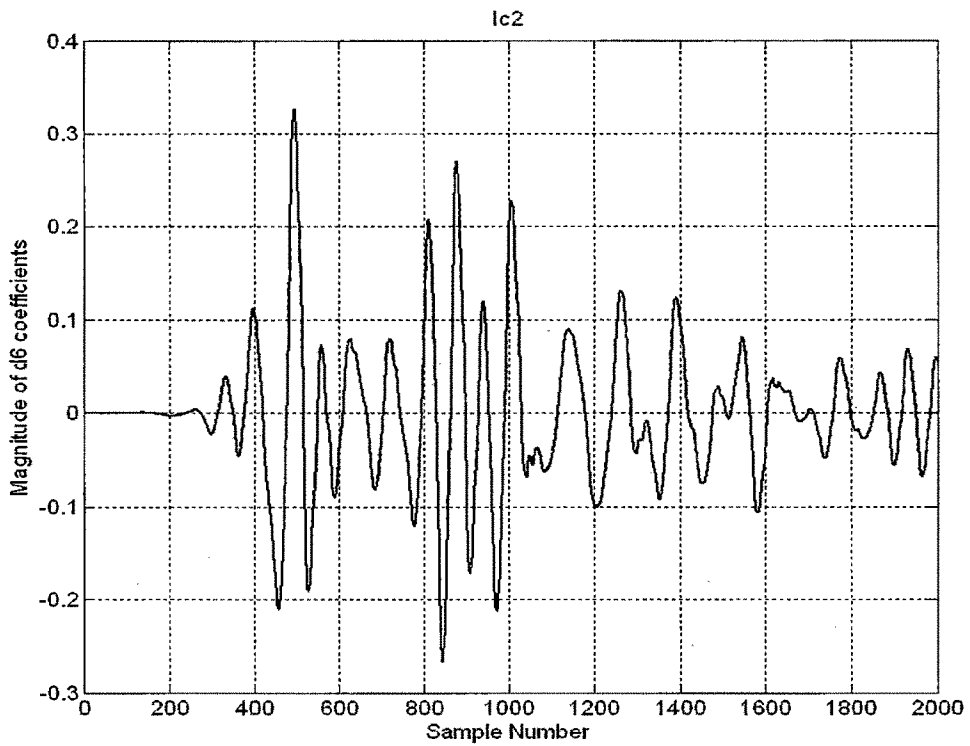
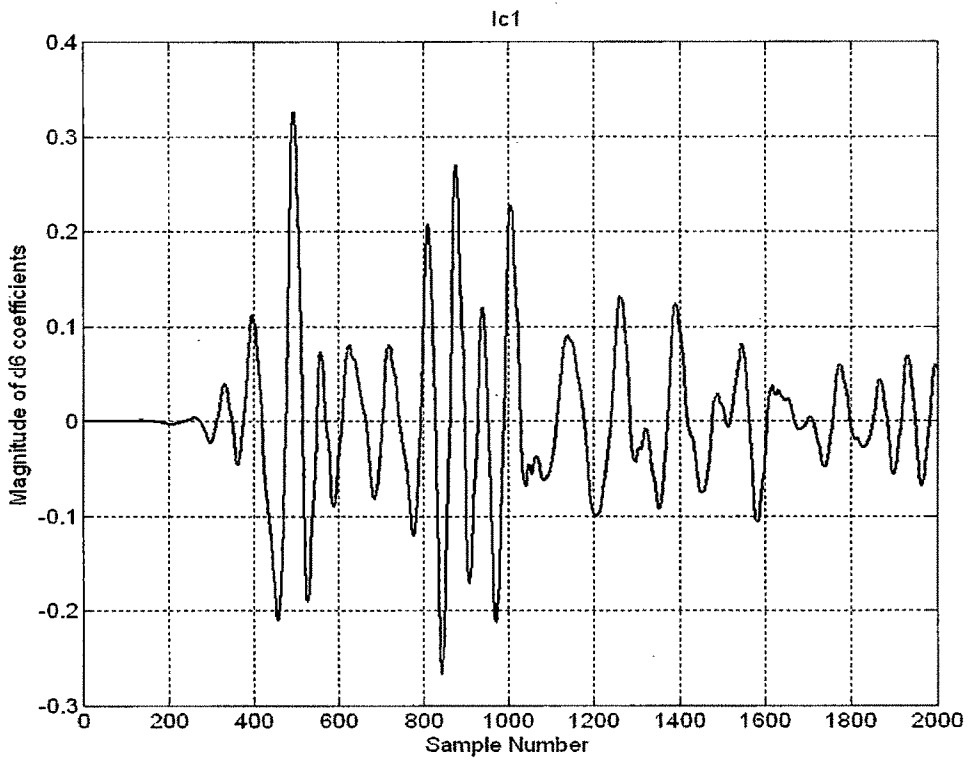


Fig.4.21 Plots showing magnitudes of fault spikes for C- Phase on both the ends for A-B External Fault

From the plots (Figure 4.19,4.20 and 4.21) it's evident that **though** the magnitude of level 6 detail coefficients is exceeding the set threshold by large extent in A,B phase, **due to identical pattern of the spikes on the both the ends of the line** the proposed scheme classifies the fault as **A-B (external fault)** and prevents tripping.

(12) $X_c=50\%$, $Z_{G1}=100\%$, $Z_{G2}=100\%$, A-B Fault between Bus-B1 and Source G1, $R_f=0.01 \Omega$ (**External Fault**)

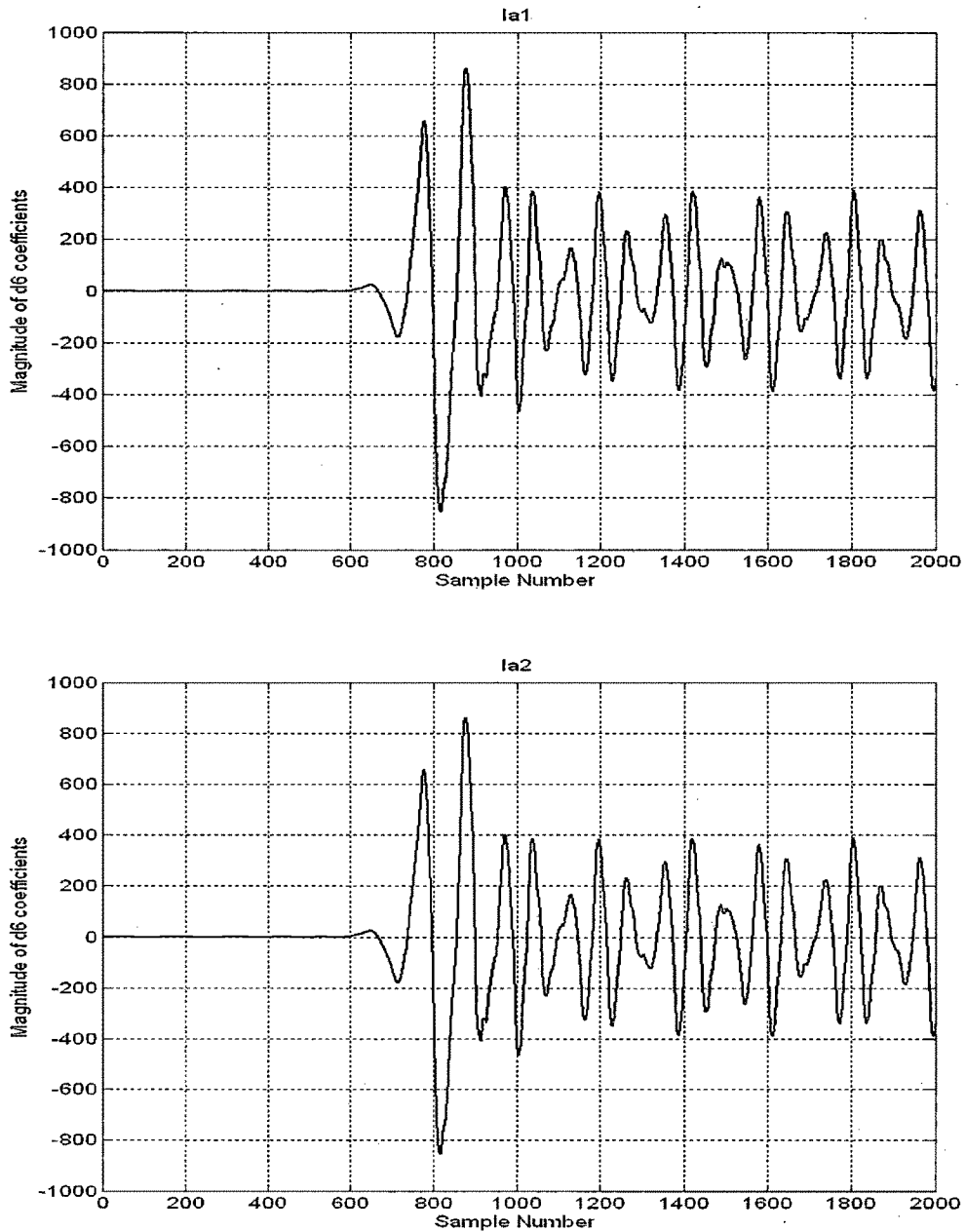


Fig.4.22 Plots showing magnitudes of fault spikes for A- Phase on both the ends for A-B External Fault

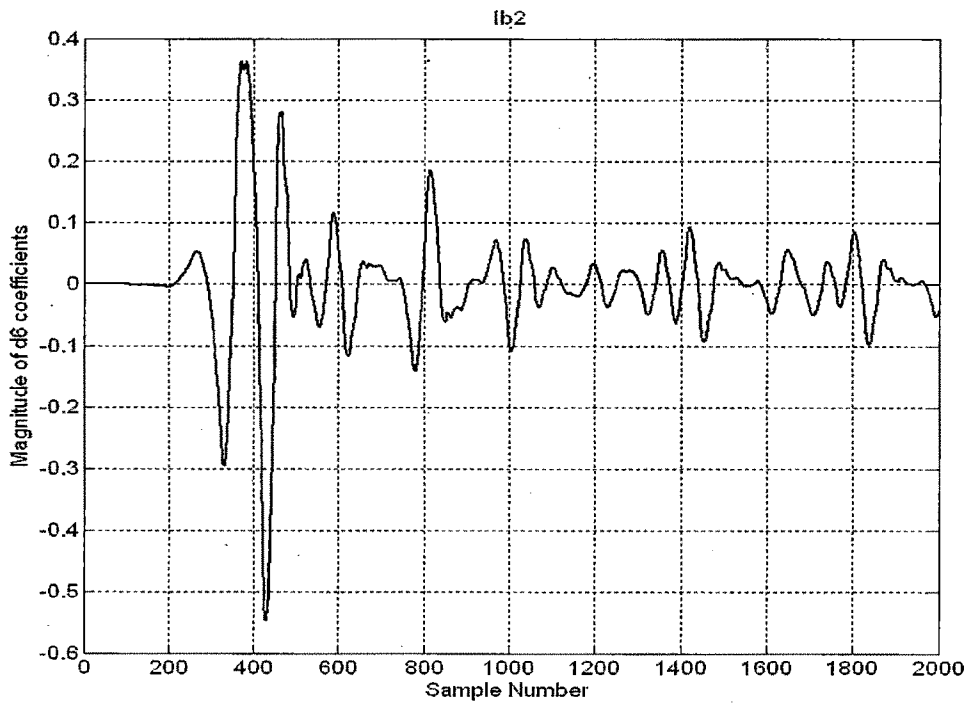
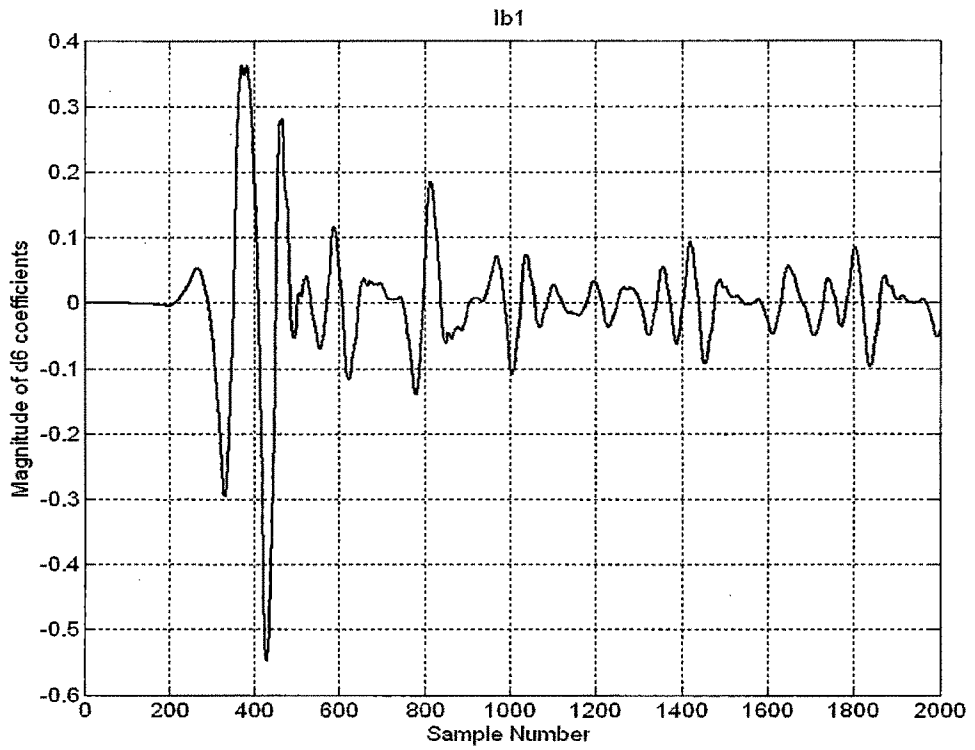


Fig.4.23 Plots showing magnitudes of fault spikes for B- Phase on both the ends for A-B External Fault

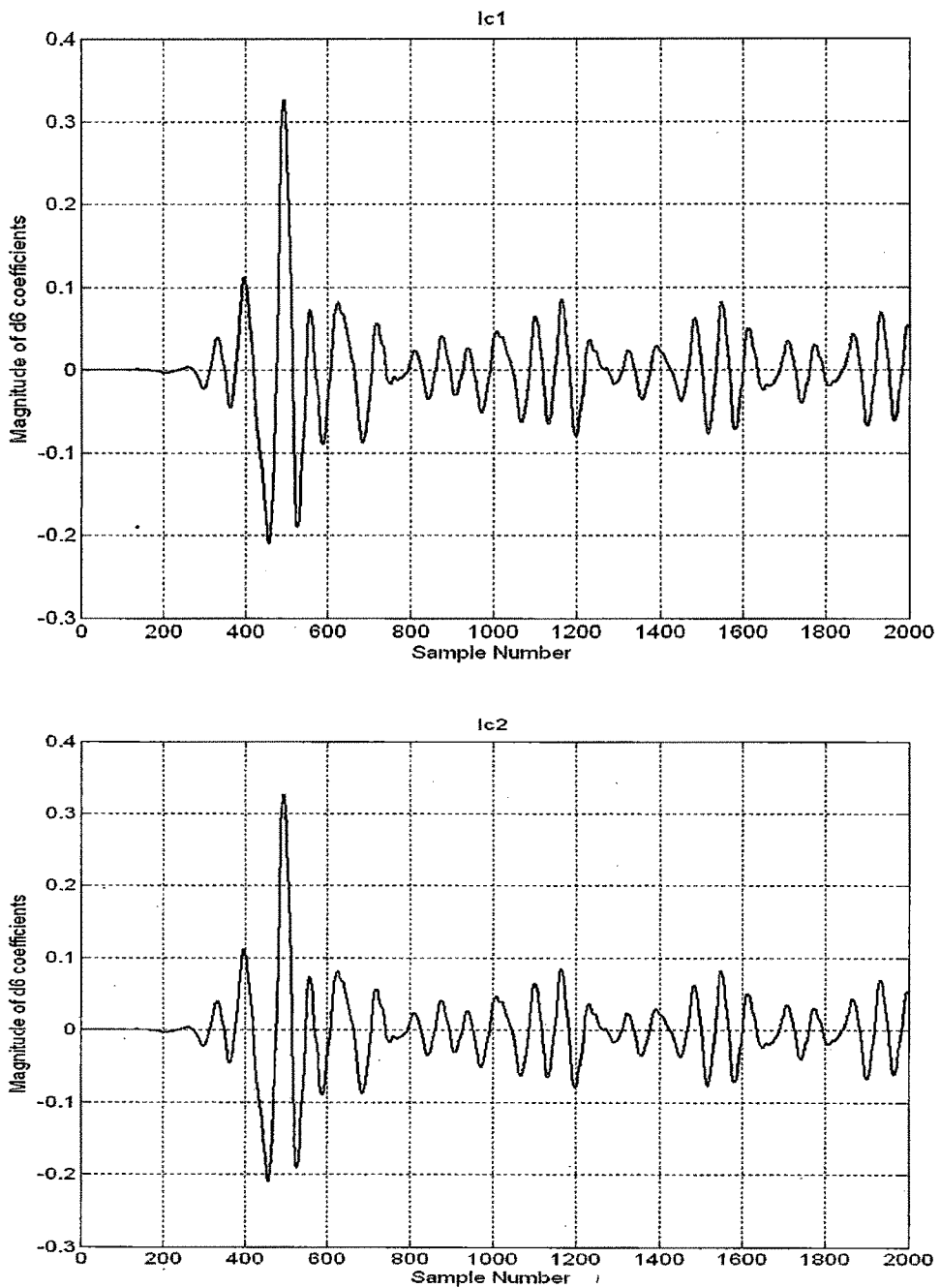


Fig.4.24 Plots showing magnitudes of fault spikes for C- Phase on both the ends for A-B External Fault

From the plots (Figure 4.22,4.23 and 4.24) it's evident that **though** the magnitude of level 6 detail coefficients is exceeding the set threshold by large extent in A,B phase, **due to identical pattern of the spikes on the both the ends of the line** the proposed scheme classifies the fault as **A-B (external fault)** and prevents tripping.

4.5 Summary of Simulation Results

The proposed scheme has been extensively tested by carrying out fault simulation studies under wide variation of load angle, fault inception angle, fault resistance and fault locations, compensation levels and variation of source impedance. A total 30,000 simulation cases (28,800 (Internal faults) , 1200 (External faults and Load switching transients)) has been tested using suggested scheme.

Table 4.3 Performance of Proposed Scheme with Different Parameters

Case No.	Xc %	ZG1 %	ZG2 %	Threshold For d6 coefficients Line currents	Threshold For d6 coefficients ground current	No. of Test Cases	True Relaying Decision	Incorrect Relaying Decision	Accuracy (%)
1	50	100	100	0.5	0.00001	2000	1944	56	97.200
2		75	100	0.5	0.00001	2000	1953	47	97.650
3		125	100	0.5	0.00001	2000	1872	128	93.600
4		100	75	0.5	0.00001	2000	1960	40	98.000
5		100	125	0.5	0.00001	2000	1888	112	94.400
6	25	100	100	0.3	0.00001	2000	1932	68	96.960
7		75	100	0.3	0.00001	2000	1947	53	97.350
8		125	100	0.3	0.00001	2000	1853	147	92.650
9		100	75	0.3	0.00001	2000	1944	56	97.200
10		100	125	0.3	0.00001	2000	1870	130	93.500
11	75	100	100	0.8	0.00001	2000	1954	46	97.700
12		75	100	0.8	0.00001	2000	1967	33	98.350
13		125	100	0.8	0.00001	2000	1893	107	94.650
14		100	75	0.8	0.00001	2000	1972	28	98.600
15		100	125	0.8	0.00001	2000	1920	80	96.000
Total						30000	28869	1131	96.230

Table 4.3 gives the thresholds selected through heuristic approach for detection of the faults for various compensation levels with variation of source impedances. It also shows the accuracy of the proposed scheme with different parameters. From Table 4.3 it can be said that the proposed technique is quite effective in case of wide variations in the source impedance along with the change in compensation level.

As proposed scheme is a unit protection technique its high performance accuracy is always guaranteed in simulation studies, However its practical performance accuracy (which will be marginally lower than the theoretical obtained through simulation studies) depends largely on the accuracy of communication channels or time synchronization methods used for obtaining the signals from remote end at the relaying decision making end.